DEVELOPMENT OF POLYMER-LIPID HYBRID NANOPARTICLES FOR ANTICANCER DRUG DELIVERY

by

Sedef Salel

B.S., in Biomedical Engineering, Bahçeşehir University, 2020

Submitted to the Institute of Biomedical Engineering
in partial fulfillment of the requirements
for the degree of
Master of Science
in
Biomedical Engineering

Boğaziçi University
2022

ACKNOWLEDGMENTS

Firstly, I would like to express my gratitude to my advisor, Dr. Banu İyisan for her support, patience and understanding throughout my master study. She always helped me to learn, give me the courage to continue even in the hardest times, and believed in me. I would also like to thank my friends Dilan Avşar Akdeniz, Gökçen Boran, Damla Kelle, Gizem Uysal, and Elif Özlem Topal for their friendship and support.

Also; I would like to thank TUBITAK for supporting me financially with 2210-A scholarship program, and Boğaziçi University Research Fund (18042) for funding this project.

Besides, I would like to express my gratitude and love to my parents Çiğdem-Mesut Uzunsakal, and my brother Emirhan Uzunsakal for their love, encouragement and constant support.

Lastly, I would especially like to express my gratitude and love to my dear husband Muharrem Salel for his constant love. He always believed in me, and supported me in any ways imaginable.

ACADEMIC ETHICS AND INTEGRITY STATEMENT

I, Sedef Salel, hereby certify that I am aware of the Academic Ethics and Integrity Policy issued by the Council of Higher Education (YÖK) and I fully acknowledge all the consequences due to its violation by plagiarism or any other way.

Name :

Signature:

Date:

ABSTRACT

DEVELOPMENT OF POLYMER-LIPID HYBRID NANOPARTICLES FOR ANTICANCER DRUG DELIVERY

The challenge of conventional cancer treatment is the side effects caused by the chemotherapeutic drugs. To prevent these side effects, nanocarrier systems can be designed to have functions of controlled and selective drug release. Among these systems, core-shell structured hybrid nanoparticles have been drawing attention in the last decades because of their multifunctional structures. The major limitations of these nanocarrier systems are the toxicity related to synthetic surfactants as well as undesired leakage of highly toxic drugs. In this study, a unique nanocarrier system was designed using natural materials for controlled delivery of an anticancer drug. This system contains a biopolymeric shell and a lipid core which could be used to encapsulate lipophilic anticancer drugs. Bovine Serum Albumin (BSA) and Dextran in different molecular weights were covalently conjugated via Maillard reaction to produce shell and used to stabilize lipid core by miniemulsion/solvent evaporation method. The shell of the nanoparticle could prevent undesired drug leakage from the core and provide enzyme-sensitive drug release thanks to its protein structure. Shell properties such as concentration of the Maillard conjugate, protein-polysaccharide molar ratio, and polysaccharide molecular weight were systematically investigated to reach optimum nanoparticle features that are size which can enable passive targeting through enhanced permeability and retention (EPR) effect, narrow size distribution, and high stability. Furthermore, zeta potential analysis was performed to evaluate surface charge of the nanoparticles in physiological (pH 7.4) and early endosomal (pH 6.5) mimicking environment. This study can bring new perspectives to the hybrid nanoparticles and has a potential to be a new delivery platform for lipophilic anticancer drugs.

Keywords: Drug Delivery Systems, Hybrid Nanoparticles, Protein-Polysaccharide Complexes

ÖZET

ANTİKANSER İLAÇ SALIMI İÇİN BİYOPOLİMER KABUK-KATI LİPİT ÇEKİRDEK YAPILI HİBRİT NANOPARTİKÜLLERİN GELİŞTİRİLMESİ

Yaygın olarak kullanılan kanser tedavilerinin en büyük dezavantajı, kanser ilaçlarının neden olduğu yan etkilerdir. Bu yan etkileri önleyebilmek için nanotaşıyıcı sistemler, kontrollü ve seçici ilaç salımı yapabilecek şekilde tasarlanabilir. Bu sistemler arasında çekirdek-kabuk yapılı hibrit nanoparçacıklar, çok işlevli yapıları nedeniyle son yıllarda dikkat çekmektedir. Bu nanoparçacıkların en önemli sorunları ise sentetik yüzey aktif maddelerden kaynaklanabilen toksik etki ve yüksek derecede etkili ilaçların ilaç taşıma sisteminden sızıntısıdır. Bu çalışmada, antikanser ilaçların kontrollü salımı için doğal malzemelerle oluşturulmuş bir nanotaşıyıcı sistem tasarlanmıştır. Bu sistem, lipofilik antikanser ilaçlarını taşımak için kullanılabilecek bir lipit çekirdek ve polimer kabuğa sahiptir. Bu çekirdek-kabuk yapılı hibrit nanoparçacığın kabuk yapısını oluşturmak için farklı moleküler ağırlıklardaki Dekstran polisakkaritleri ile Sığır Serum Albumini proteini, Maillard reaksiyonu kullanılarak kovalent bağ ile bağlanmış ve miniemülsiyon/çözücü buharlaştırma yöntemi ile lipit çekirdeği kararlı hale getirmek için kullanılmıştır. Ayrıca kabuk yapısı, istenmeyen ilaç sızıntılarını da önleyebilir ve protein yapısı sayesinde enzime duyarlı ilaç salımı sağlayabilir. Maillard kompleksleri konsantrasyonu, protein-polisakkarit molar oranı ve polisakkarit moleküler ağırlığı gibi kabuk özellikleri sistematik olarak değiştirilerek, bu çalışma için optimum nanoparçacık özelliklerine ulaşılmıştır. Bu özellikler, gelişmiş geçirgenlik ve tutma etkisi yoluyla pasif hedeflemeyi sağlayabilecek bir boyut, dar boyut dağılımı ve yüksek kararlılık olarak verilebilir. Ayrıca, nanoparçacıkların fizyolojik (pH 7.4) ve erken endozom (pH 6.5) koşullarındaki yüzey yükünü gözlemlemek için zeta potansiyeli analizleri yapılmıştır. Bu çalışma, hibrit nanopartiküllere yeni bakış açıları getirmiş ve lipofilik antikanser ilaçları için yeni bir dağıtım platformu oluşturma potansiyeline sahiptir.

Anahtar Sözcükler: İlaç Salım sistemleri, Hibrit Nanopartiküller, Protein-Polisakkarit Kompleksleri

TABLE OF CONTENTS

LIST OF FIGURES

LIST OF TABLES

LIST OF SYMBOLS

°C	Celcius
μg	Microgram
μl	Microliter
mg	Milligram
mV	Millivolt
M	Molar
nm	Nanometer

LIST OF ABBREVIATIONS

ACS	American Chemical Society
BSA	Bovine Serum Albumin
DLS	Dynamic Light Scattering
EPR	Enhanced Permeability and Retention
FTIR	Fourier Transform Infrared Spectroscopy
GC	Gas Chromatography
LLPN	Liquid Lipid-Polymer Hybrid Nanoparticle
MW	Molecular Weight
NLC	Nanostructured Lipid Carrier
NP	Nanoparticle
SDS-PAGE	Sodium Dodecyl Sulfate-Polyacrylamide Gel Electrophoresis
SEM	Scanning Electron Microscopy
SLN	Solid Lipid Nanoparticle
SLPN	Solid Lipid-Polymer Hybrid Nanoparticle
STEM	Scanning Transmission Electron Microscopy

1. INTRODUCTION

1.1 Motivation

There is a need for nano-sized carrier systems to make controlled drug release that can be effective in tumor cells and to eliminate the side effects of chemotherapy by preventing drugs from damaging healthy cells [1]. Hybrid nanocarrier systems created using natural materials could release drugs with minimum side effects, and could provide a safer, controlled, and targeted delivery of the drugs to cancerous cells. The hybrid core-shell structure of the nanoparticles in this thesis is expected to prolong the drug release time by trapping the drug in the lipid core, prevent initial burst release, and cause less damage to healthy cells compared to conventional drugs.

Based on the information given, the motivation behind this thesis is to produce a unique hybrid nanoparticle design with a biopolymer shell and a lipid core which could carry highly lipophilic anticancer drugs and provide controlled drug delivery.

1.2 Objectives

The main purpose of this study is designing a novel hybrid nanocarrier system using natural materials for controlled delivery of a lipophilic drug. To achieve this purpose, the following steps will be followed respectively: (i) A natural biopolymeric shell will be obtained by forming a complex from a mixture of protein (bovine serum albumin) and polysaccharide (dextran) through Maillard reaction. (ii) Hybrid nanocarrier systems will be obtained by combining the shell and lipid core by applying miniemulsion/solvent evaporation method. (iii) The physicochemical and morphological properties of the hybrid nanoparticles will be examined by various characterization methods.

1.3 Thesis Outline

This thesis is divided into 5 chapters.:

Chapter 1 gives the motivation, objectives, and outlines of this thesis.

In Chapter 2, background information about nanocarriers for drug delivery applications, lipid nanoparticles, hybrid nanoparticles, surfactants and anticancer drugs is given.

Chapter 3 explains the materials and methods used in this thesis. Methods are divided into four subsections as preparation of shell using BSA-dextran complexes, characterization of complexes, fabrication of hybrid nanoparticles, and characterization of the nanoparticles.

The results of the experiments and characterization techniques, and their discussions are given in Chapter 4.

Finally, conclusions of this research and future works are given in Chapter 5.

2. RESEARCH BACKGROUND

2.1 Nanoparticles for Drug Delivery Applications

Drug delivery field is developing rapidly with the increasing knowledge in Biomedical Engineering, Bioengineering, and Nanotechnology [2]. Many novel delivery systems benefit from nanotechnology to carry bioactive agents [3]. The main aim of nanotechnology for drug delivery field is the same with the medicine field: early diagnosis and efficient therapy by minimizing side effects [4]. For these purposes many nanostructured materials are created such as carbon nanotubes, iron oxide nanoparticles, gold nanoparticles, mesoporous silica nanoparticles, liposomes, dendrimers, micelles, quantum dots, lipid nanoparticles, polymer nanoparticles, and hybrid nanoparticles (Figure 2.1) [5].

In cancer nanomedicine field, when the appropriate nanocarrier type is selected, the appropriate identification methods for the cancer cells should be decided. There are certain physicochemical differences between cancerous and healthy cells. Smart drug delivery systems benefits from these differences to recognize cancer areas. As an example of these differences, pH value (lower in cancer sites), enzymatic activities (catalytically-active proteins up-regulated (increase with an outside stimulation) in

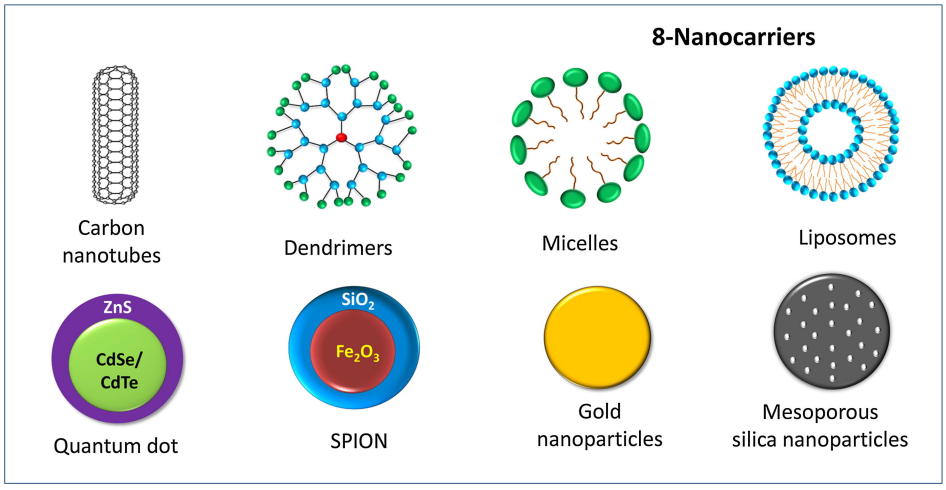

Figure 2.1 Representative figure of eight nanoparticle types used for drug delivery [5].

cancer sites), redox status (intra- and extracellular glutathione (GSH) concentrations are different), and temperature values (higher in cancer sites) could be given [7]. For the identification of the cancer cell sites, there are two main strategies: passive targeting and active targeting. Passive targeting benefits Enhanced Permeability and Retention (EPR) effect to indirectly target tumor sites. EPR effect is the enhanced permeability of cancer cells because of the hypervasculature around tumor tissues (Figure 2.2) [8]. Active targeting is achieved by interactions between various receptors that are over-

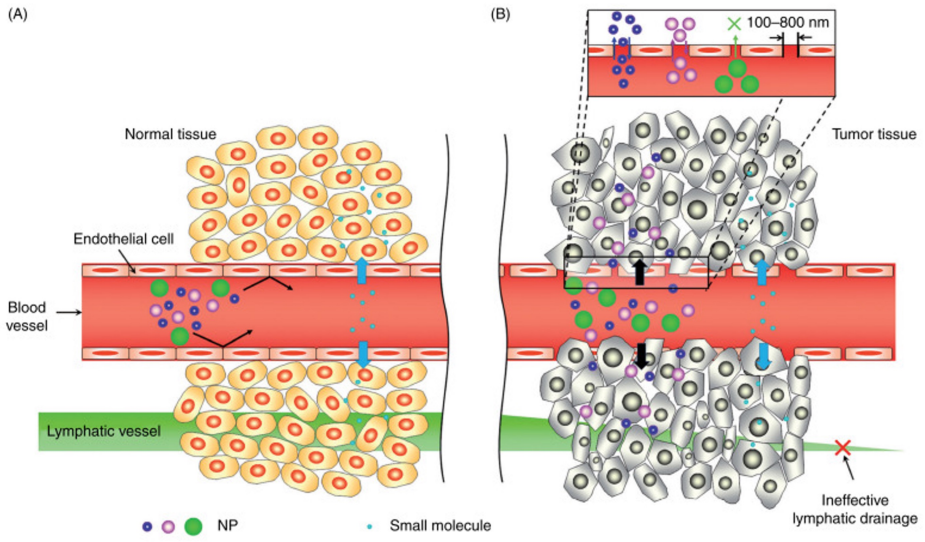

Figure 2.2 Representative image of differential uptake of nanoparticles and small molecules based on their size across (A) normal and (B) cancerous tissues [6]

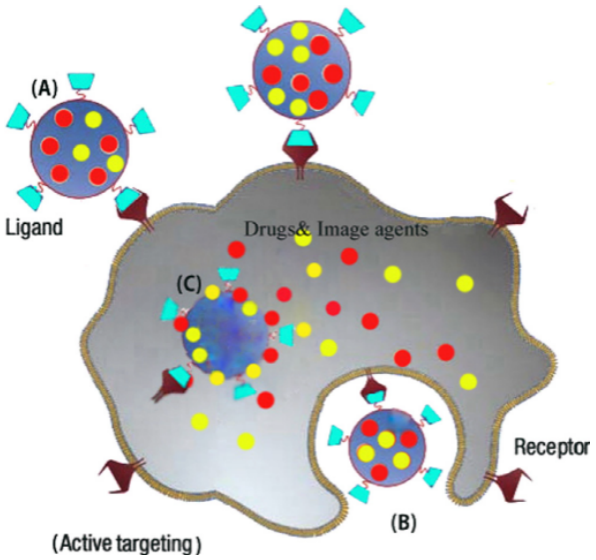

Figure 2.3 Representative image of active targeting operation that nanoparticles transmit drugs and image agents to the targeted cells. (A) Receptor-ligand interactions; (B) Receptor-mediated endocytosis; (C) Release of the drugs and image agents into the targeted cell [6]

expressed in cancer cells and ligands which are attached to nanoparticle surfaces to be attracted to corresponding receptors (Figure 2.3) [6].

2.2 Lipid Nanoparticles

Lipid nanoparticles could be divided into two categories as solid lipid nanoparticles (SLNs) and nanostructured lipid carriers (NLCs). SLNs (Figure 2.4) first created in 1991 as an alternative nanocarriers to the traditional colloid particles such as liposomes, emulsions, and polymer nanostructured materials [9]. They are advantageous as they have superior biocompatibility, high loading capacity, ability to carry both hydrophilic and hydrophobic bioactive molecules, enhanced drug stability, ease in production than biopolymer nanocarriers [10]. One disadvantages of the SLNs is that hardening and following crystallization of the solid lipid cause the leakage of the encapsulated drugs which leads to instability in the long-term [11]. This is based on the condition which lipid particles crystallize rapidly in more stable states and cause particle size incrementation and loading capacity reduction [12]. Nanostructured Lipid Carriers (NLCs) contain both solid and liquid lipids mixed in the nanoparticles which are solid in room and body temperature [14]. NLCs solve the size increase and loading capacity reduction limitations of SLNs because a high quantity of drugs can be loaded in defects of the nanocarrier preventing the rapid release of the drugs and leading to

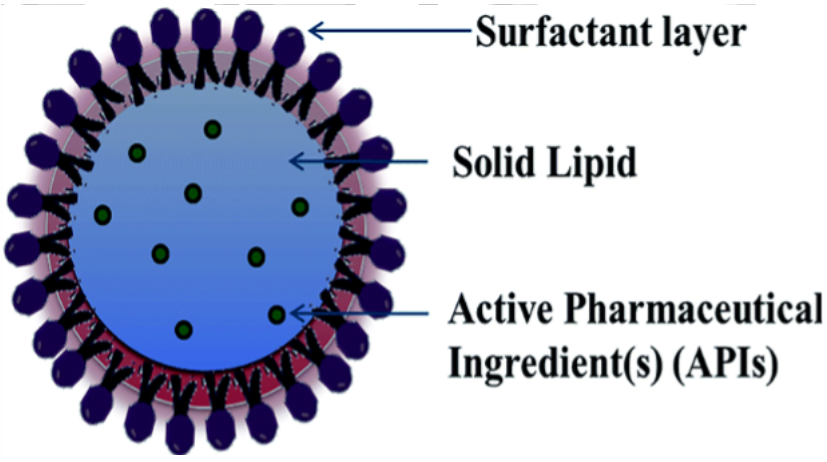

Figure 2.4 Representative image of the SLNs structure [13]

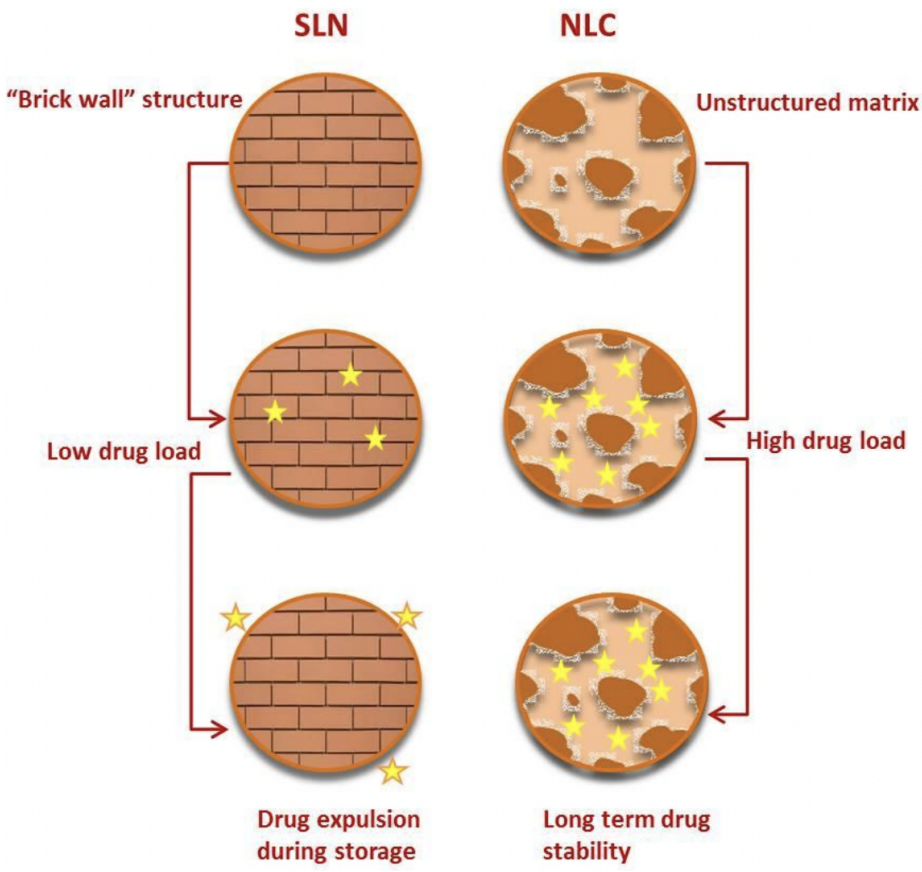

Figure 2.5 Representative image of Solid Lipid Nanoparticles (SLNs) and Nanostructured Lipid Carriers (NLCs), where NLC advantages over SLNs are emphasized [17]

a better loading capacity [15]. Besides, NLCs provide better stability than SLNs because their liquid lipid parts are preventing recrystallization of the solid parts and it ensures that the size stays almost the same while storing the nanoparticles for long times (Figure 2.5) [16].

2.3 Hybrid Nanoparticles

Amongst many nanocarrier designs, hybrid nanoparticles with core-shell structure have attracted attention in recent years due to their multifunctional structure [18, 19]. Hybrid nanoparticles can be used in fields such as remote optical sensing, fluorescent imaging, photodynamic therapy, and controlled drug release systems [20, 21] Many of the core-shell hybrid nanoparticle designs for drug delivery are made using a polymer core and a lipid shell. However, this design has some disadvantages such

as low colloidal stability in the gastrointestinal tract and persistent aggregation from lyophilization when high amounts of surfactant (up to 60% by weight of lipid-polymer hybrid nanoparticle) are not used before freeze drying (lyophilization) [22]. Using a lipid core and biopolymeric shell, instead of polymeric core-lipid shell design, provides the nanoparticle to have high drug-carrying capacity and remarkable stability thanks to stabilizing properties of protein-polysaccharide conjugates [23] [24]. Moreover, in hybrid nanoparticles, the lipid core provides superior encapsulation ability for highly lipophilic drugs [23]. On the other hand, the biopolymeric shell increases the stability of the nanoparticles, and protects the drug which is trapped in the nanoparticle core during blood circulation against external factors [25].

2.4 Surfactants and Other Stabilizers

Surfactant could also be called as Surface-Active Agent (Figure 2.6). It is an amphiphilic compound (includes both hydrophilic (polar)(head) and hydrophobic (non-polar)(tail) parts) which could be used as detergent, wetting agent, or emulsifier [26]. Thanks to their amphiphilic structure, surfactants decrease the surface tension between a liquid and a solid, a liquid or a gas. Surfactants are categorized according to charges of their hydrophilic head portion [27]. There are four different surfactant types: anionic, cationic, nonionic, and zwitterionic. Anionic surfactants have negatively charged head portion and they are divided to subgroups as carboxylate, sulfonate, sulfate, and phosphate. Cationic surface-active agents have positively charged head portion and generally Nitrogen atoms carry the charge. Nonionic surfactants have no charge on their head portion, and they are generally ethoxylated surfactants. Zwitterionic surfactants are also called amphoteric surfactants and they include two opposite charged active parts, they could be anionic, nonionic, anionic–cationic, or nonionic–cationic [28].

Moreover, instead of synthetic surfactants, protein-polysaccharide complexes could be used as stabilizers for emulsions [24]. Proteins are valuable in terms of their adsorption capability to lipid particles in water phase and their emulsion stabilizing features [30]. Also, most polysaccharides have emulsion stabilizing properties since

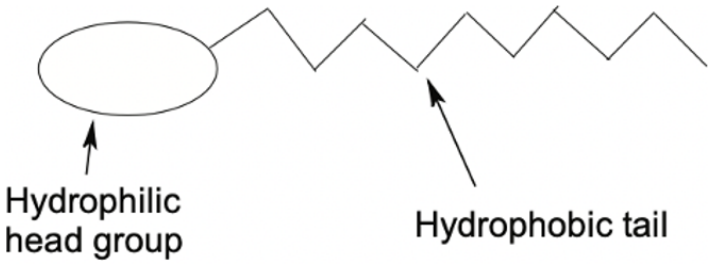

Figure 2.6 Representative figure of a surface active agent [29]

they can form an extensive net structure and increase the viscosity of the continuous phase [31]. Uniting these valuable features of proteins and polysaccharides under convenient conditions such as protein-polysaccharide molar ratio, pH, concentration, and temperature could be very beneficial for stabilizing emulsions. Proteins and polysaccharides could form a complexation with both electrostatic attractions and covalent conjugation. In this thesis, covalent conjugation of a protein and a polysaccharide were used to stabilize oil in water emulsions.

2.5 Anticancer Drugs

Main treatments for cancer include surgery, chemotherapy, and radiotherapy [32]. Chemotherapy uses small-molecule drugs to selectively kill tumor cells or least ways limit their reproduction. These anticancer drugs can be categorized by their action mechanisms such as antimetabolites, anti-tubulin agents, and DNA interactive agents. Paclitaxel was selected to be used as an anticancer drug to be encapsulated in the lipid core of fabricated nanoparticles in future studies of this thesis. It is an example of antitubulin agents which interfere with microtubule dynamics, prevent cell division and cause to cell death [33].

Paclitaxel (Figure 2.7) is originally derived from the bark of the Pacific yew tree (Taxus brevifolia) by Research Triangle Institute (North Carolina, USA) researchers Wani and Wall in 1967 [34]. It is the initial taxane used in cancer therapy and it is one of the most effective drugs used in cancer treatments [35]. It is known that this drug disrupts the normal microtubule dynamics, stops cells at the G2/M stage and triggers cell death in proliferating cancer cells, causing a highly effective reduction in ovarian,

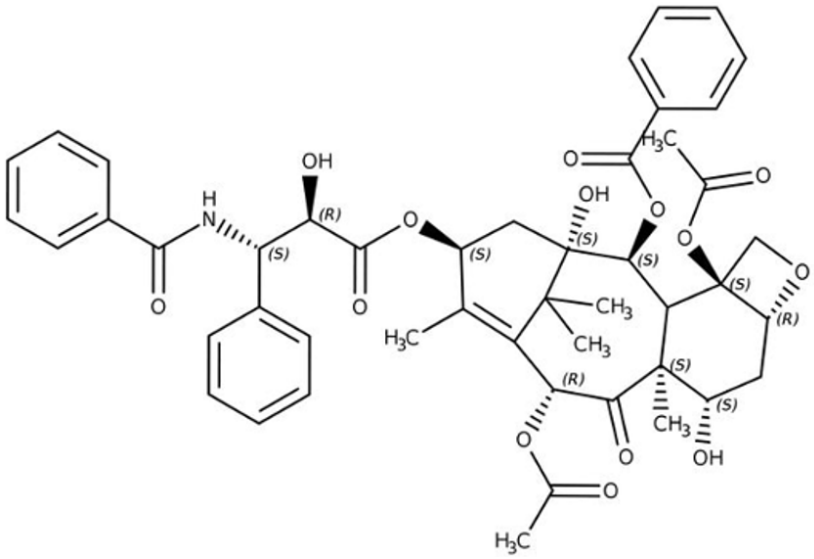

Figure 2.7 Chemical Structure of Paclitaxel [36]

breast, lung, pancreatic and brain cancer cells. The disadvantage of paclitaxel is its low water solubility which makes administration difficult.

Taxol® drug could be given as examples of Paclitaxel drugs used in the clinic [37, 38]. In 1984, researchers at John Hopkins announced that the Taxol drug showed partial or complete reactions in 30% of advanced ovarian cancer patients and in 1992, the drug was approved by FDA. Also, Taxol's effectiveness against advanced breast cancer was proved by researchers and it is approved by FDA for breast cancer treatments in 1994 [39]. Paclitaxel is dissolved with Cremofor EL (polyoxyethylated castor oil) and ethanol (1:1) in Taxol drug. Besides its significant impacts, this drug has many side effects caused by Cremofor EL such as peripheral neuropathy, hypotension, and hypersensitivity [33]. Because of the stated problems of commercial drugs, scientists continue to work on more advanced nanocarrier systems composed of lipids, biopolymers, or synthetic polymers [40–42].

3. METHODS

3.1 Materials

Bovine Serum Albumin (BSA) (purity: >98%), olive oil (highly refined, low acidity) (purity (GC area %): C18:1 oleic acid), beeswax, and hydrochloric acid (HCl) were provided from Sigma-Aldrich Company. Dextran 10 (MW:9000 to 11000), Dextran 40 (MW: 35000 to 45000), and Dextran 70 (MW: 64000 to 76000) were purchased from Carbosynth. Ethyl acetate (ACS grade) solvent used in dissolving beeswax, potassium bromide (KBr), potassium chloride (KCl), and sodium hydroxide (NaOH) were bought from Acros Organics.

SDS-PAGE materials; 4X Bolt^{TM} LDS sample buffer, 10X Bolt^{TM} reducing agent, 20X Bolt^{TM} MES SDS running buffer, Bolt^{TM} Bis-Tris running gels (10 %, 10-well), and Invitrogen^{TM} SimplyBlue^{TM} safestain (Coomassie Brilliant Blue) were acquired from ThermoFisher Scientific. Also, Pierce^{TM} 660 nm protein assay reagent was bought from Thermofisher.

For preparation of pH 6.5 and pH 7.4 phosphate buffers to mimic early endosomal and physiological conditions, monobasic sodium phosphate ($NaH_2PO_4.H_2O$) and dibasic sodium phosphate ($Na_2HPO_4.7H_2O$) was purchased from Acros Organics.

3.2 Preparation of BSA-Dextran Complexes

BSA-Dextran complexes were prepared by conducting Maillard reaction (Figure 3.1) which is the complex reaction between proteins and reducing carbohydrates with the help of heat [48]. During Maillard reaction, glucose units of dextran are covalently conjugated with amine groups of BSA protein, and produce N-substituted glycosylamine. Then it turns into Shiff base which is an unstable compound. Lastly, Schiff base turns into final Amadori product with Amadori rearrangements (Figure 3.2). A previously used method was modified for conjugation as follows [49]. BSA-Dextran

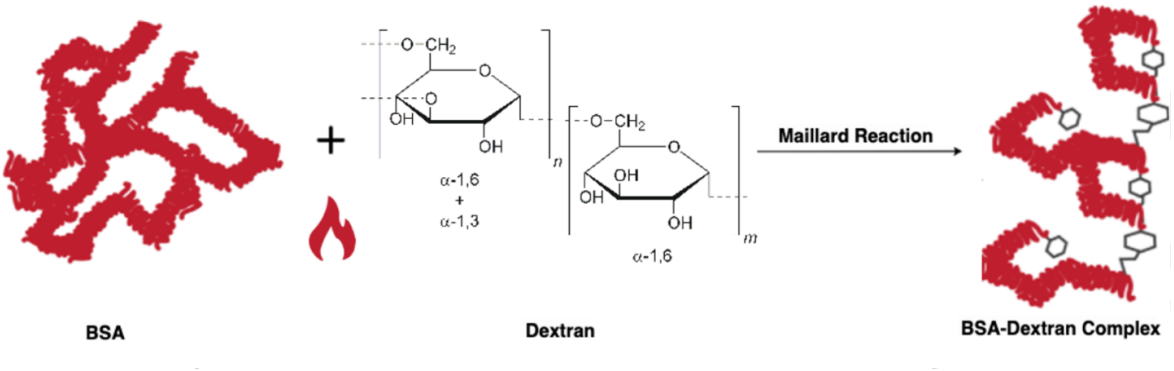

Figure 3.1 Schematic representation of preparation of BSA-Dextran complexes with Maillard Reaction.

Table 3.1 Specifications of Maillard Conjugates

Group	Molar Ratio of BSA to Dextran			Molecular Weight of Dextran (kDa)
	1:1	2:1	3:1	
BSA-Dextran10	BSA:Dex10.1	BSA:Dex10.2	BSA:Dex10.3	10
BSA-Dextran40	BSA:Dex40.1	BSA:Dex40.2	BSA:Dex40.3	40
BSA-Dextran70	BSA:Dex70.1	BSA:Dex70.2	BSA:Dex70.3	70

mixtures in molar ratios from 1:1 to 4:1 was prepared using total amount of 100 mg BSA and Dextran and 10 ml water. The mixtures were stirred for 16 hours. The pH of the mixture was adjusted to 8 using 0.1 M Sodium Hydroxide (NaOH), followed by 24 hours lyophilization in a Christ Alpha 1-4 Lyophilizer. Then, the freeze-dried solution was put to incubator inside a desiccator containing saturated Potassium Bromide (KBr) solution to provide 79% relative humidity for 48 hours at 60 °C. The resulted products were specified as Maillard conjugates and stored in 4 °C. The groups and molar ratios of Maillard conjugates can be seen in Table 3.1.

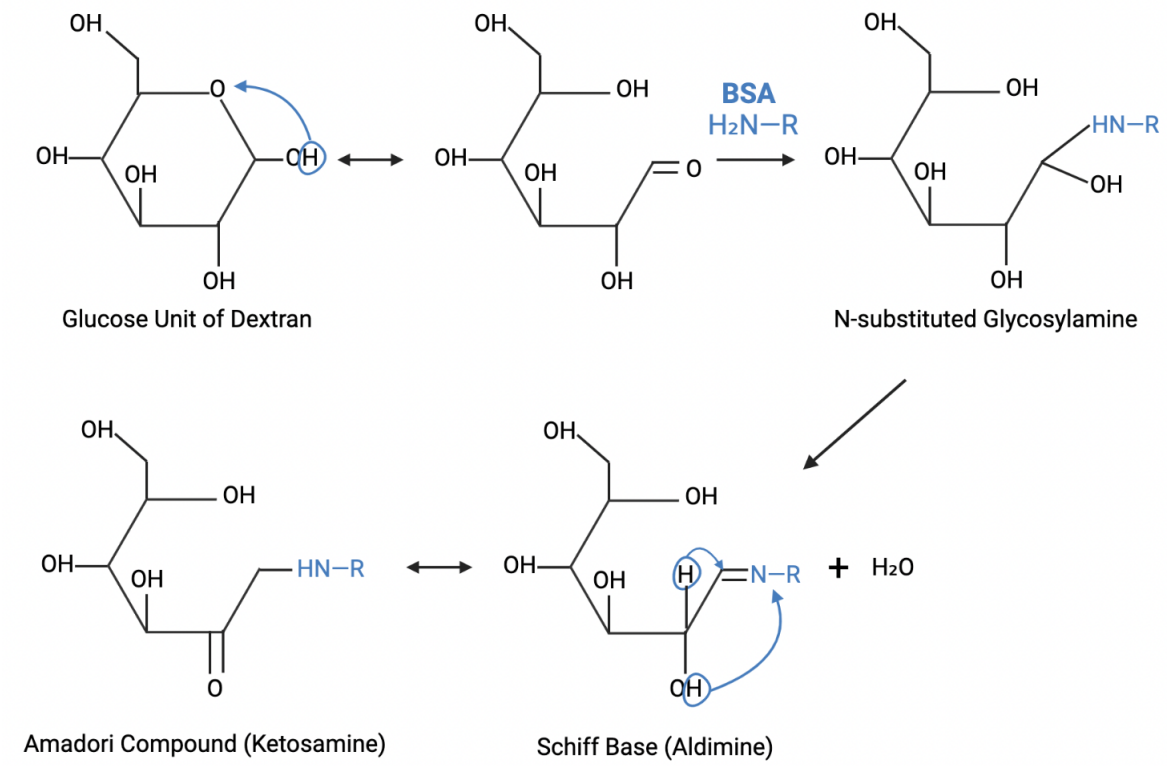

Figure 3.2 Schematic representation of Maillard reaction between BSA and dextran. Adapted from [35].

3.3 Characterization of BSA-Dextran Complexes

Fabricated BSA-Dextran Maillard conjugates were characterized by protein assay, SDS-PAGE, and FT-IR Spectroscopy. Details of performed characterization techniques for Maillard complexes are given below.

3.3.1 Protein Assay

Thermo Scientific Pierce 660 nm Protein Assay was choosen for the characterization of BSA-Dextran complexes, since it is an easy to use, quick colorimetric method and it is more linear than Bradford assays. BSA was used as the standard for the calibration curve (Figure A.1). The assay was performed in microplate. To perform the assay, firstly 1 mg/ml sample solutions were prepared using distilled water. Then, 10 μL of each replicate of standard, unknown sample, and the appropriate blank sample (distilled water) were added into a microplate well (96 well-plates). 150 μL of the

assay reagent was added to each well. The plate was shaken in medium speed for one minute and then the absorbances were measured in 655 nm. Later, distilled water absorbances were subtracted from the sample absorbances and the protein concentration of each sample were calculated according to the constituted calibration curve. Each absorbance measurement was taken three times.

3.3.2 Sodium Dodecyl Sulfate-Polyacrylamide Gel Electrophoresis (SDS-PAGE)

SDS-Page was performed to confirm Maillard conjugation between BSA and Dextran in prepared complexes. Each conjugate was dissolved in distilled water at a concentration of 1 mg/ml. 0.5 mg/ml BSA solution and the conjugate samples were prepared for loading according to sample preparation protocol (Table 3.2) and heated at 70 °C for 10 minutes in a block heater. After running buffer loaded, BSA and each samples were loaded to wells as each sample well contains 2.5 μg BSA. SDS-Page was performed at 40 mA for 90 minutes. The gels were stained by Coomassie Brilliant Blue solution overnight and rinsed in 200 mL distilled water for 1 hour twice. The gels were then scanned and pictured using a scanner (Bio-Rad Gel Doc XR+ Gel Documentation System). Pictures of each stage of the SDS-PAGE could be seen in Figure 3.3 below.

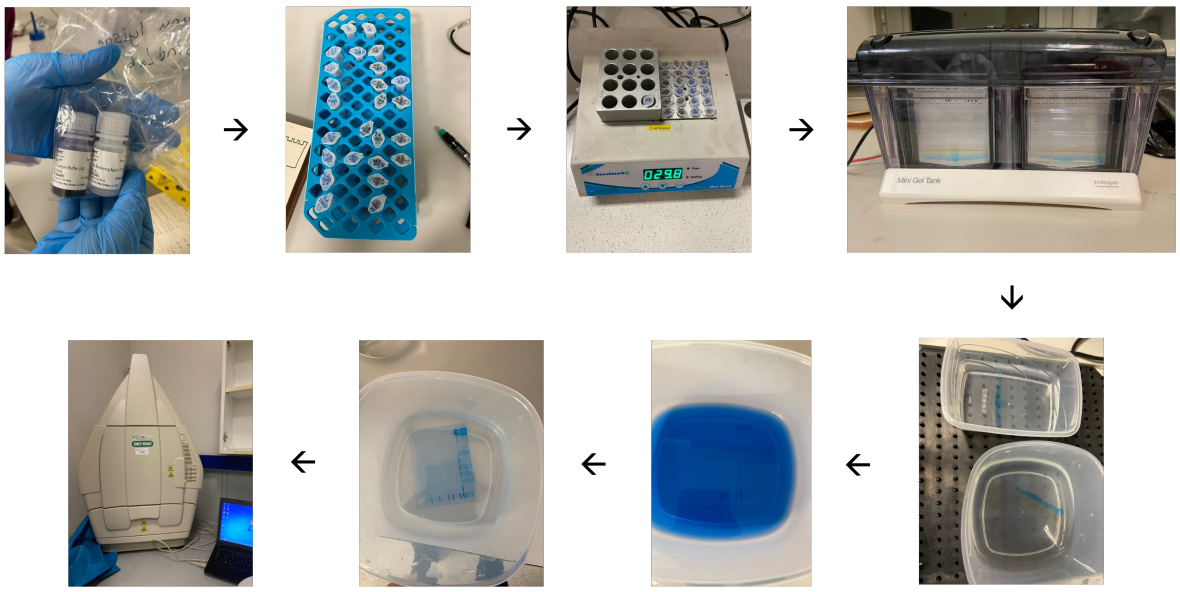

Figure 3.3 SDS-PAGE Procedure

Table 3.2 SDS-PAGE Sample Preparation Protocol

Materials	**Amount**
Sample	x µl (independent variable)
4X Bolt™ LDS Sample Buffer	2.5 µl
10X Bolt™ Reducing Agent	1 µl
Distilled Water	up to 6.5 µl
Total Volume	10 µl

3.3.3 Fourier Transform-Infrared Spectroscopy (FT-IR)

FT-IR spectroscopy (Thermo Scientific Nicolet 380 FT-IR spectrometer) was used to understand the chemical properties and structures of BSA, Dextran and their Maillard complexes. It was performed in Chemistry Department at Boğaziçi University and the spectroscopy results were taken in the range of 400 cm^{-1} to 4000 cm^{-1}. To obtain FT-IR spectrums; firstly, background was measured. Then, 2 mg of native BSA, Dextran10, Dextran40, Dextran70, and their Maillard complexes were put to FT-IR spectrometer and their measurements were performed. Finally, the data were organized to be able to investigate the differences between the samples.

3.4 Fabrication of Biopolymeric Shell-Lipid Core Nanoparticles

Hybrid nanoparticles with a biopolymeric shell and a solid lipid core were formed by direct (oil-in-water) miniemulsion-solvent evaporation method (Figure 3.4). In this method, nanoparticles are formed by dispersing the preformed polymeric solution in an aqueous environment with a hydrophobic phase that contains the lipid core components, and the desired miniemulsion is obtained by evaporating the solvent in the solution [43]. While most of the studies use synthetic surfactants to stabilize nanoparticles; in this study, stabilization was obtained with produced natural biopolymeric shell. For SLPNs; Olive oil (60 mg), beeswax (40 mg) and ethyl acetate solvent (2 ml) were used as dispersed phase in oil-in-water emulsion, while bovine serum albumin-dextran

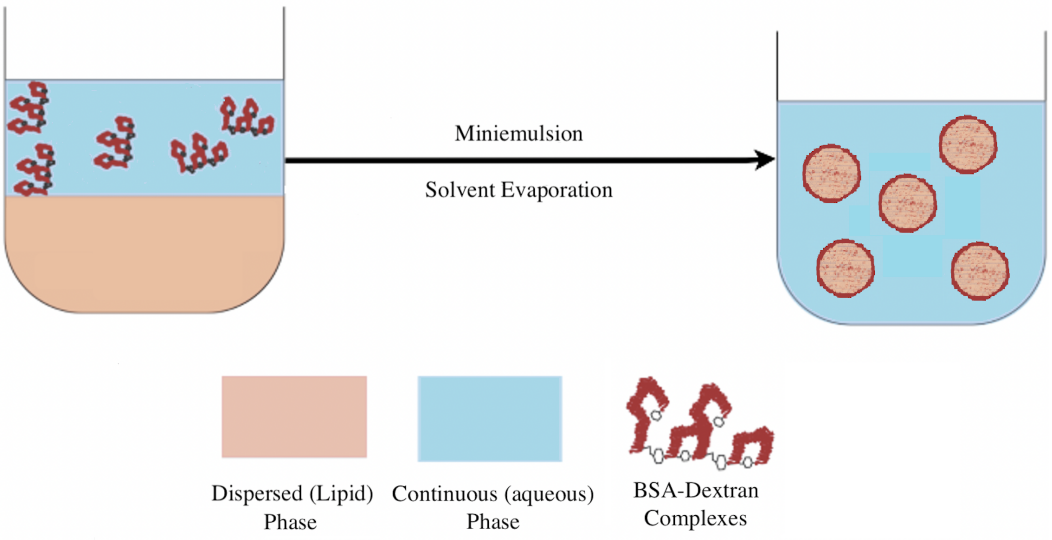

Figure 3.4 Schematic representation of hybrid nanoparticle production with miniemulsion-solvent evaporation method.

complexes (1 mg/ml) were used as continuous phase (10 ml). For LLPNs; Olive oil (100 mg) was used as dispersed phase in oil-in-water emulsion, while bovine serum albumin-dextran complexes (1 mg/ml) were used as continuous phase (10 ml). Then, these two phases were mixed and stirred at 1000 rpm for 10 minutes, and ultrasonication was carried out for 4 minutes under an ice bath at 90% amplitude for 15 seconds on and 5 seconds off (Branson 550 Sonifier, Boğaziçi University). The ethyl acetate solvent was evaporated by stirring the dispersion at room temperature at 300 rpm for 16 hours. Specifications of the nanoparticles are given in Table 3.3 below.

3.5 Characterization of Nanoparticles

Fabricated nanoparticles were characterized in terms of their solid contents, size, PDI, zeta potential, and morphology. Details of performed characterization techniques of nanoparticles are given below.

Table 3.3 Specifications of Fabricated Nanoparticles

Nanoparticle	**Core-Lipid Content (%wt)**	**Shell-BSA:Dextran Maillard Conjugate**	**Nanoparticle Shell Related Specifications**
SLPN10	Beeswax (40%) Olive Oil (60%)	BSA;Dex10.1 BSA;Dex10.2 BSA;Dex10.3	SLPN10.1 SLPN10.2 SLPN10.3
SLPN40	Beeswax (40%) Olive Oil (60%)	BSA;Dex40.1 BSA;Dex40.2 BSA;Dex40.3	SLPN40.1 SLPN40.2 SLPN40.3
SLPN70	Beeswax (40%) Olive Oil (60%)	BSA;Dex70.1 BSA;Dex70.2 BSA;Dex70.3	SLPN70.1 SLPN70.2 SLPN70.3
LLPN10	Olive Oil (100%)	BSA;Dex10.1 BSA;Dex10.2 BSA;Dex10.3	LLPN10.1 LLPN10.2 LLPN10.3
LLPN40	Olive Oil (100%)	BSA;Dex40.1 BSA;Dex40.2 BSA;Dex40.3	LLPN40.1 LLPN40.2 LLPN40.3
LLPN70	Olive Oil (100%)	BSA;Dex70.1 BSA;Dex70.2 BSA;Dex70.3	LLPN70.1 LPN70.2 LLPN70.3

3.5.1 Solid Content Analysis

Solid content amounts of each fabricated nanoparticles were measured. Measurements were performed by firstly placing 100 µl nanoparticle dispersions to three different centrifuge tubes and weighing the dispersions and subtracting each centrifuge tube's weights. Then, each dispersion in the centrifuge tubes were freeze-dried and remaining solids were weighted to calculate the solid content amounts of each dispersion.

3.5.2 Size and Polydispersity Index (PDI) Measurements

Size and PDI measurements of the nanoparticles were obtained using Dynamic Light Scattering device (Malvern Zetasizer Nano ZS, Boğaziçi University) (Figure 3.5.a). The measurements were taken at an angle of 173° and in 25 °C temperature. The dispersions were diluted 10 times for obtaining approximately 1 mg/ml solid content. For the measurements, square glass cuvette with square aperture and cap (12 mm optical density) (Figure 3.5.b) was used.

3.5.3 Zeta Potential Analysis

Zeta potential measurements of the nanoparticles were obtained using Dynamic Light Scattering device (Malvern Zetasizer Nano ZS, Boğaziçi University) (Figure 3.5.c). In the same way as size and PDI measurements; zeta potential measurements were taken at an angle of 173° and in 25 °C temperature. The dispersions were 10 times diluted with 1 mM potassium chloride solution. For the measurements, disposable folded capillary zeta cell was used.

(a) (b) (c)

Figure 3.5 (a) Dynamic Light Scattering Device (b) Square glass cuvette with square aperture and cap for size measurements (c) Disposable folded capillary cell for zeta potential analysis.

3.5.4 Morphological Characterization

Scanning Transmission Electron Microscopy (STEM) was used to observe the morphology of selected nanoparticle (SLPN10.1). 3 µL sample was dried on a 300-grid copper mesh for 30 minutes prior to morphology observation using a Scanning Electron Microscopy (SEM) device (Thermo Scientific Quattro S, Boğaziçi University Lifesci).

4. RESULTS and DISCUSSION

4.1 Characterization Results of BSA-Dextran Complexes

BSA-Dextran Maillard conjugates were characterized with three different methods which are;

(1) Protein assay,

(2) Sodium Dodecyl Sulfate-Polyacrylamide Gel Electrophoresis (SDS-PAGE),

(3) Fourier Transform-Infrared Spectroscopy (FT-IR).

The results of these characterization techniques are given below.

4.1.1 Protein Assay

Protein Assay results of the Maillard conjugates could be seen in Table 4.1. The results showed that protein concentrations of the Maillard conjugates were between 330 to 630 μg/ml, and they were adequate for shell of the nanoparticles.

4.1.2 Sodium Dodecyl Sulfate-Polyacrylamide Gel Electrophoresis (SDS-PAGE)

In Figure 4.1; the SDS-PAGE results of BSA-Dextran10, BSA-Dextran40, and BSA-Dextran70 conjugates could be seen. As seen from the figure, BSA showed a clear and thick band around molecular weight 70 kDa, which was expected since native BSA has 66.5kDa molecular weight. Besides, BSA also showed two other smear bands at higher molecular weights which could be because of the aggregates of BSA monomers during heating operation of sample preparation for SDS-PAGE.

Table 4.1 Protein Assay Results of BSA-Dextran Conjugates. Protein concentrations were given as the average of three results.

Sample	Absorbance (a.u.)	Protein Concentration (μg/ml)
BSA:Dex10.1	0.174	356
BSA:Dex10.2	0.163	334
BSA:Dex10.3	0.296	600
BSA:Dex40.1	0.282	572
BSA:Dex40.2	0.309	626
BSA:Dex40.3	0.179	366.6
BSA:Dex70.1	0.228	444
BSA:Dex70.2	0.253	513.3
BSA:Dex70.3	0.215	438

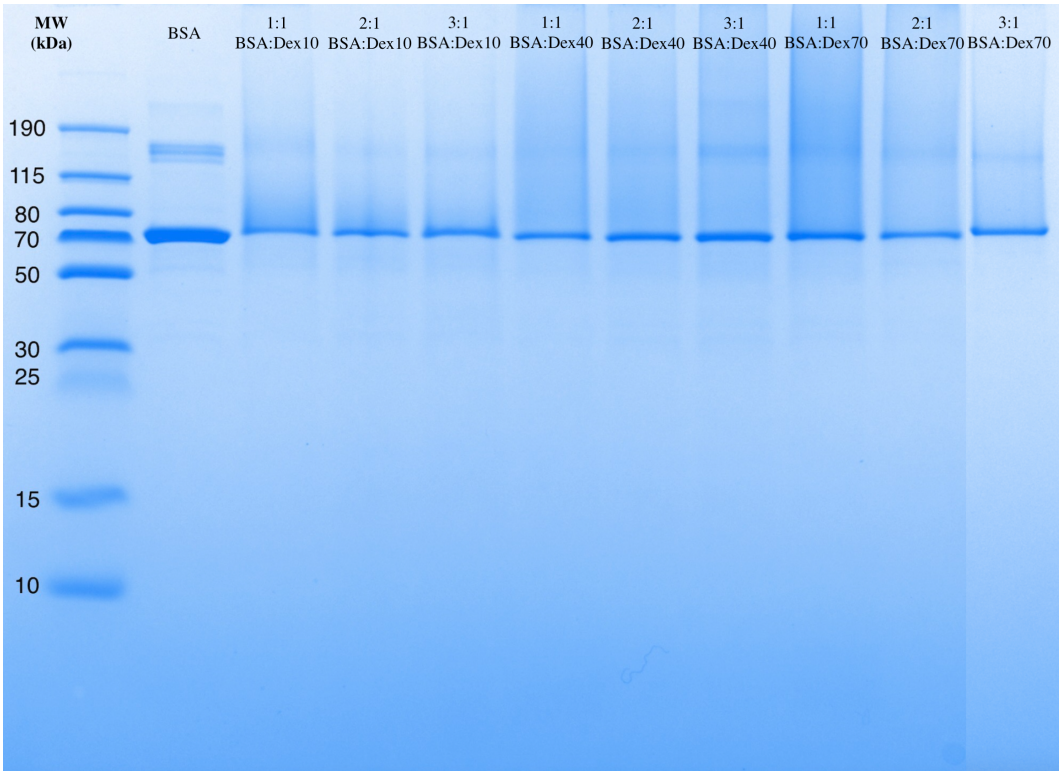

Figure 4.1 SDS-Page results of only BSA, BSA-Dextran10 conjugates, BSA-Dextran40 conjugates, and BSA-Dextran70 conjugates. The molar ratios were given above each conjugates name in the figure.

4.1.3 Fourier Transform-Infrared Spectroscopy (FT-IR)

In the FT-IR spectrums below two major characteristic peaks of BSA which corresponds to Amide 1 and Amide 2 stretching vibrations could be seen around wave-

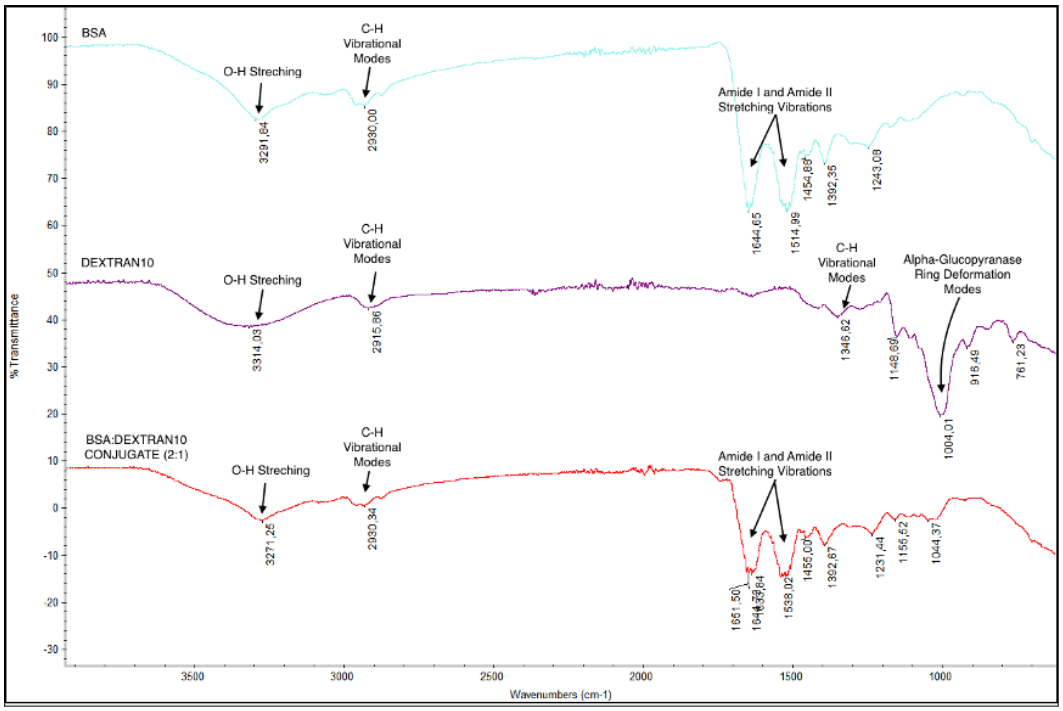

Figure 4.2 FT-IR Spectrum of: BSA (blue), Dextran10 (MW:9000-11000 kDa) (purple), BSA-Dex10.2 (red).

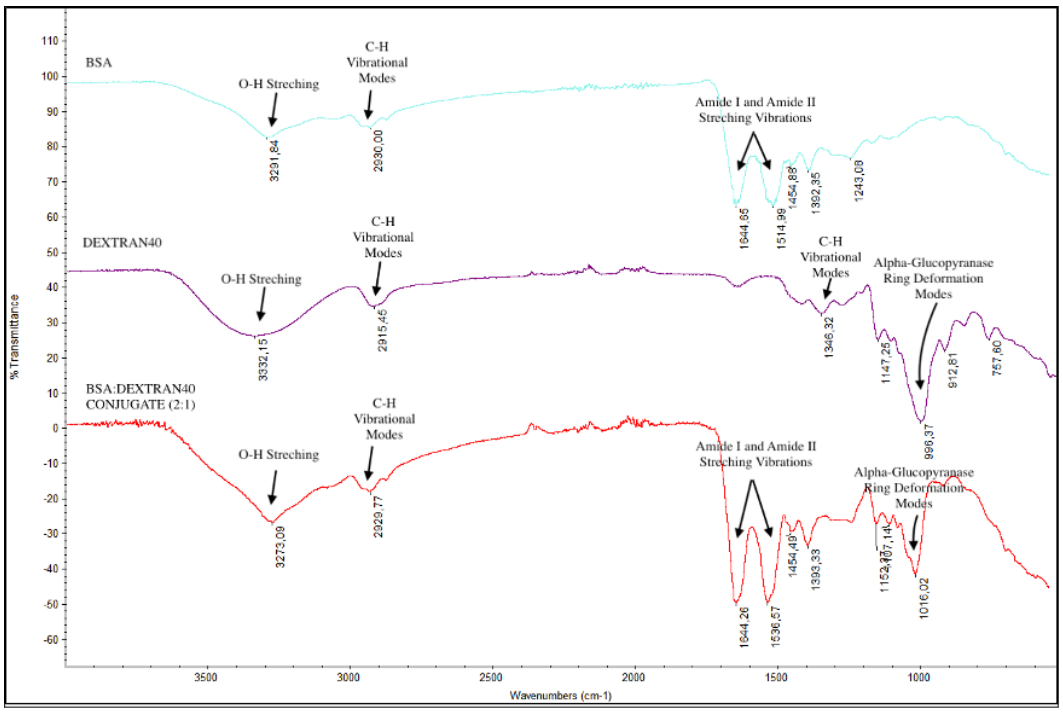

Figure 4.3 FT-IR Spectrum of: BSA (blue), Dextran40 (MW:35000-45000 kDa) (purple), BSA-Dex40.2 (red)

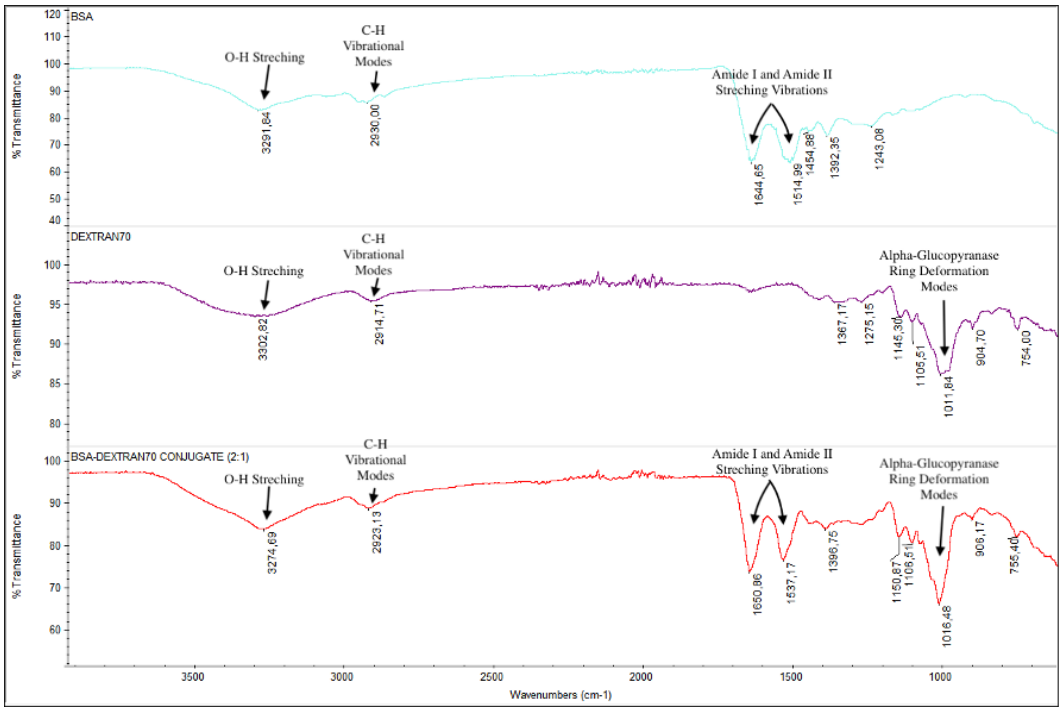

Figure 4.4 FT-IR Spectrum of: BSA (blue), Dextran70 (MW:64000-76000 kDa) (purple), BSA-Dex70.2 (red)

length 1650 and 1520, respectively (Fig. 4.2-4.4 (blue)) [1]. Each dextran spectrum (Fig. 4.2-4.4 (purple)) showed characteristic polysaccharide bands comprising O-H stretching region around wavelength 3300, and alpha-glucopyranase ring deformation modes between 700 and 1010 wavelengths [35, 44]. BSA-dextran Maillard conjugates (Fig. 4.2-4.4 (red)) displayed significantly sharp peaks at the amide stretching region of 1500–1650 cm-1, indicating the successful formation of new amide bonds between BSA and Dextran molecules [45].

4.2 Characterization Results of the Hybrid Nanoparticles

Characterization results of the fabricated hybrid nanoparticles are divided into five subsections which are (1) size and polydispersity index measurements, (2) selection of the optimum nanoparticle design, (3) stability test results, (4) zeta potential analysis, and (5) morphological characterization.

4.2.1 Size and Polydispersity Index Measurements

Size and size distributions of the fabricated nanoparticles were investigated in five different experiments each having different conditions.Results of these experiments are given below in four subsections. Nanoparticle sizes and polydispersity indices were analysed against various temperature, dextran molecular weight, BSA-Dextran molar ratio, BSA-Dextran conjugate concentration, and purification.

4.2.1.1 Temperature Effect on Nanoparticle Size and Polydispersity

Continuos phase and dispersed phase of each group were ultrasonicated for nanoparticle fabrication. Ultrasonication was performed in two different condition to observe the effects of temperature on average nanoparticle size and polydispersity index (PDI) (Table 4.2). First condition was using ice to cover sample vials during ultrasonication, and the second was ultrasonication without ice covering the vial. It was observed that using ice during ultrasonication and preventing temperature increase was resulted in smaller sizes and PDIs in nanoparticles (Figure 4.5). Bigger sizes and PDIs of the nanoparticles with no ice usage could be due to denaturation of BSA protein caused by high temperature which leads to insufficient shell structure.

Table 4.2 Temperature effect on nanoparticle size and PDI.

Nanoparticle	**Ice Usage to Prevent Temperature Increase on NP Production**	**Average Size (nm)**	**Polydispersity Index**
SLPN10.1	Yes	229.6±3.3	0.340±0.019
SLPN10.1	No	397.7±20.2	0.511±0.095
SLPN40.1	Yes	240.8±1.5	0.350±0.006
SLPN40.1	No	273.6±7.3	0.453±0.049
SLPN70.1	Yes	253.3±3.8	0.239±0.012
SLPN70.1	No	539.0±23.8	0.547±0.013

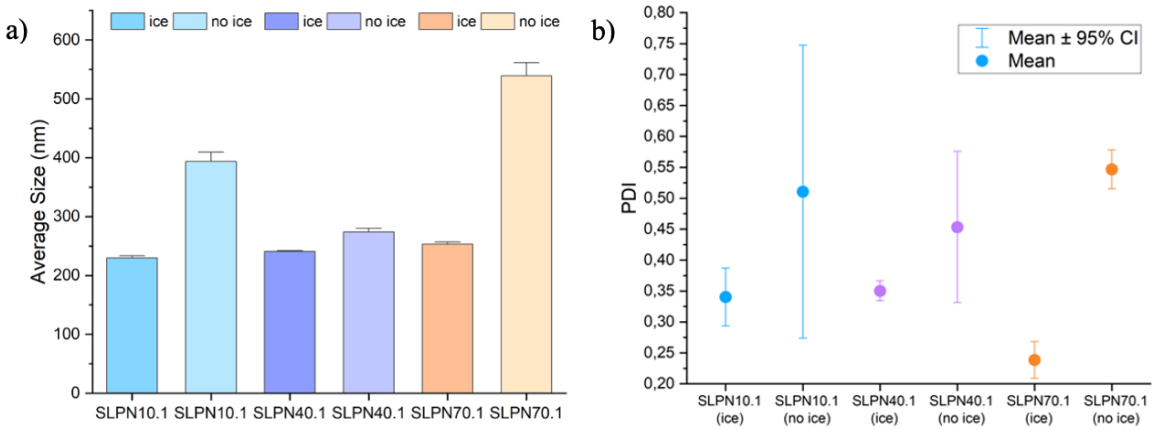

Figure 4.5 Graphs of Temperature Effect on a) Nanoparticle Size b) PDI.

4.2.1.2 Dextran Molecular Weight and BSA-Dextran Molar Ratio Effect on Nanoparticle Size and Polydispersity

For the shell of the nanoparticles, different molecular weighted dextran was used in the Maillard conjugates to test the changes in average size and PDI of the nanoparticles (Table 4.3, Table 4.4). As the molecular weight of dextran increases, average size of the SLPNs were increased (Figure 4.6.a). However, the polydispersity index of the SLPNs was not significantly affected by dextran molecular weight changes (Figure 4.6.b). The average sizes and PDIs of LLPNs were also not significantly affected by dextran molecular weight changes (Figure 4.7). Moreover; it could be seen that average size and PDI values of LLPNs were higher than SLPNs values which could mean that SLPNs have higher affinity for BSA-Dextran complexes because of the presense of beeswax (solid lipid) in the core.

Moreover, BSA-Dextran Maillard conjugates molar ratio dependent changes in nanoparticles average sizes and PDI are given below in Table 4.5, and their corresponding graphs could be seen in Figure 4.8. Average sizes were between 200 to 260 and PDIs were between 0.240 to 0.276. There was no significant difference between different molar ratios of BSA:Dextran.

Table 4.3 Dextran Molecular Weight Effect on Solid Lipid-Polymer Hybrid Nanoparticle Size and PDI

Nanoparticle	Average Size (nm)	Polydispersity Index
SLPN10.1	217.0±2.2	0.258±0.009
SLPN40.1	240.8±1.5	0.350±0.006
SLPN70.1	253.3±3.8	0.239±0.012

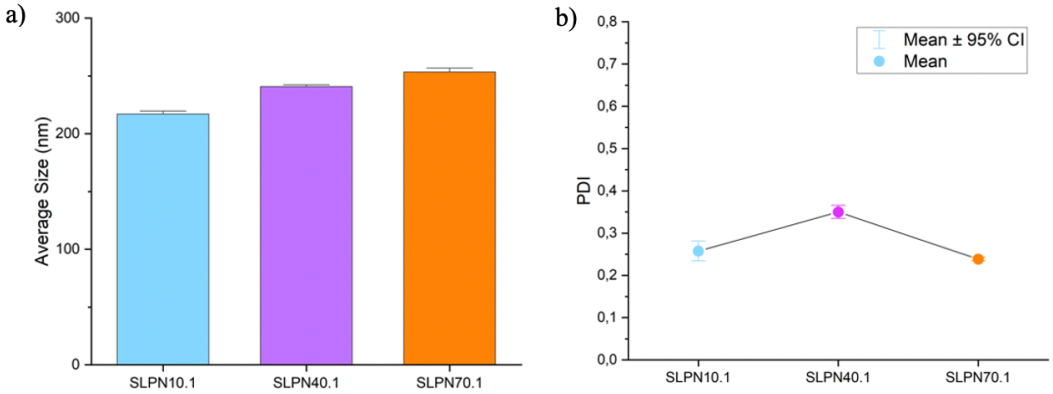

Figure 4.6 Graphs of Dextran Molecular Weight Effect on Solid Lipid-Polymer Hybrid Nanoparticle a) Size b) PDI.

Table 4.4 Dextran Molecular Weight Effect on Liquid Lipid-Polymer Hybrid Nanoparticle Size and PDI

Nanoparticle	Average Size (nm)	Polydispersity Index
LPN10.1	244.5±2.2	0.371±0.030
LPN40.1	330.6±9.1	0.479±0.023
LPN70.1	299.9±3.8	0.357±0.018

Table 4.5 BSA-Dextran Molar Ratio Effect on Nanoparticle Size and PDI

Nanoparticle	BSA-Dextran Molar Ratio	Average Size (nm)	Polydispersity Index
SLPN10.1	1:1	217.0±2.2	0.258±0.009
SLPN10.2	2:1	256.6±2.9	0.275±0.004
SLPN10.3	3:1	235.7±2.6	0.243±0.010

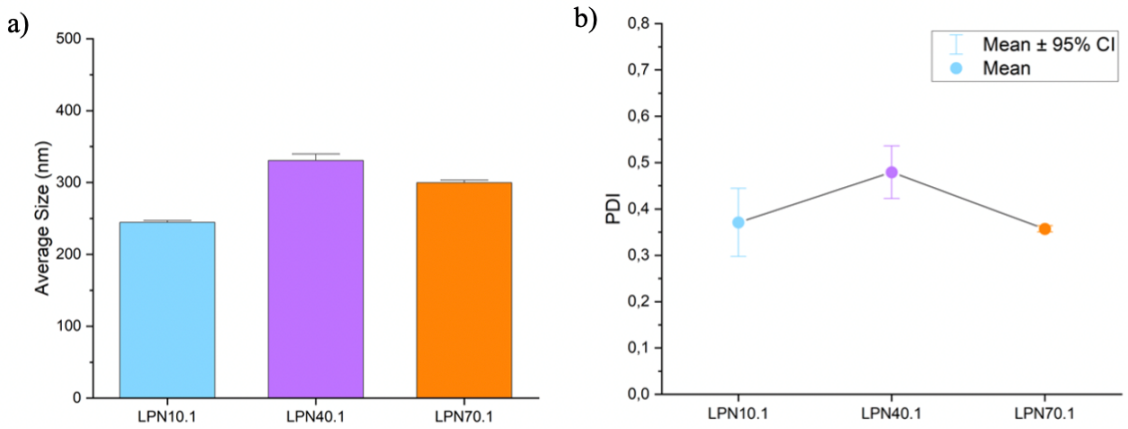

Figure 4.7 Graphs of Dextran Molecular Weight Effect on Liquid Lipid-Polymer Hybrid Nanoparticle a) Size b) PDI.

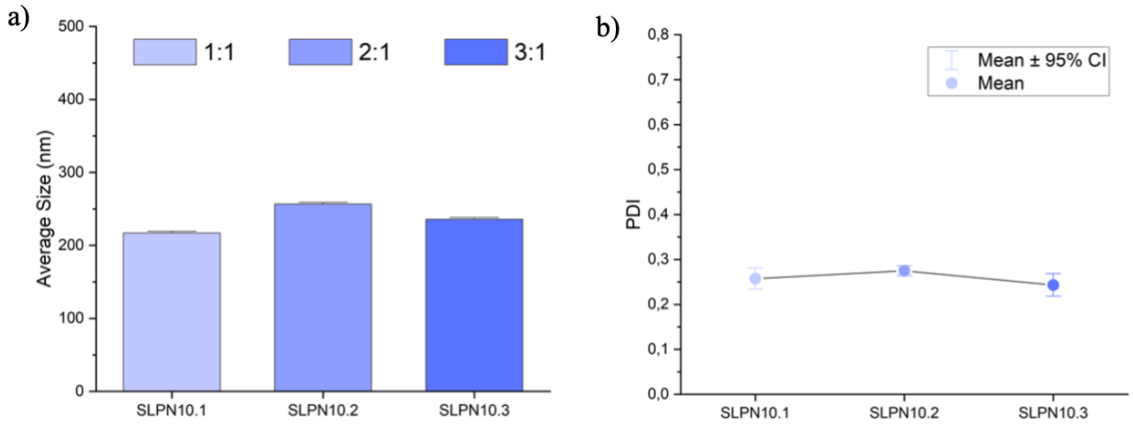

Figure 4.8 Graphs of BSA-Dextran Molar Ratio Effect on Nanoparticle a) Size b) PDI.

4.2.1.3 BSA-Dextran Conjugate Concentration Effect on Nanoparticle Size and Polydispersity

Effects of BSA-Dextran conjugate concentration changes in SLPN and LLPN average size and PDI are given below in Table 4.6 and Table 4.7. As BSA-Dextran conjugates concentration was increased in the emulsion, SLPN10.1 average size were slightly increased (Figure4.9.a). However, its PDI were decreased (Figure 4.9.b). LLPNs average size and PDI were bigger than SLPNs. SLPN average sizes were between 210 to 230, and PDIs were between 0.170 to 0.260. LLPN average sizes were between 280 to 455, and PDIs were between 0.330 to 0.500 (Figure 4.10).

The reason of obtaining smaller PDI values when BSA:Dextran maillard conjugate concentration were increased could be that the density of continuous phase of the emulsions was increased and the complexes could more effectively cover the core surface of the nanoparticles. So that, a better emulsification and stabilization was performed in higher concentrations of maillard conjugates. Furthermore, it has been proven again that SLPNs were resulted with smaller sizes and PDI values than LLPNs. After this characterization results, the nanoparticles including both solid and liquid lipid in the core were chosen to continue to the next characterizations of this study.

Table 4.6 BSA-Dextran Conjugate Concentration Effect on Solid Lipid-Polymer Hybrid Nanoparticle Size and Polydispersity Index (Nanoparticle: SLPN10.1)

BSA-Dextran Concentration	Average Size (nm)	Polydispersity Index
1 mg/ml	217.0±2.2	0.258±0.009
3 mg/ml	220.0±1.6	0.237±0.003
4 mg/ml	222.7±5.7	0.223±0.003
6 mg/ml	227.3±2.0	0.171±0.028

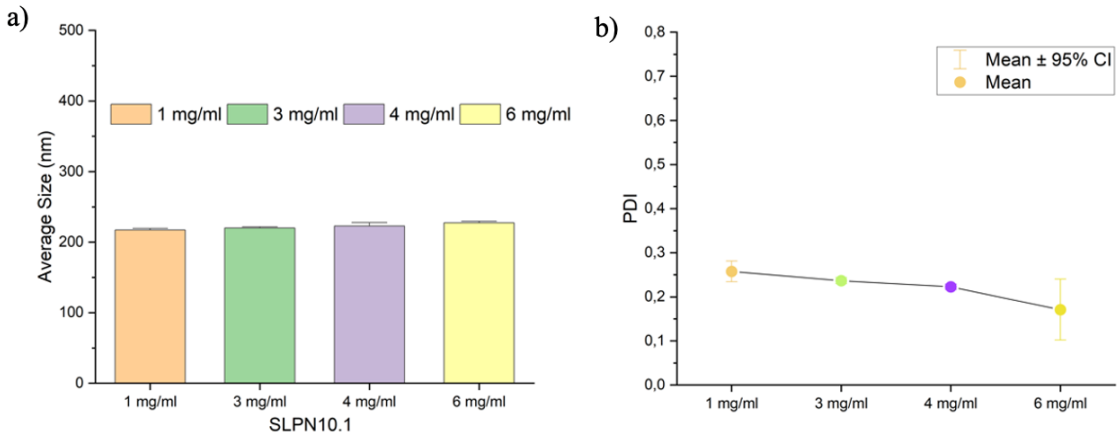

Figure 4.9 Graphs of BSA-Dextran Conjugate Concentration Effect on Solid Lipid-Polymer Hybrid Nanoparticle a) Size b) PDI.

Table 4.7 BSA-Dextran Conjugate Concentration Effect on Liquid Lipid-Polymer Hybrid Nanoparticle Size and PDI (Nanoparticle: LLPN10.1)

BSA-Dextran Concentration	Average Size (nm)	Polydispersity Index
1 mg/ml	450.8±5.3	0.479±0.007
2 mg/ml	286.8±6.4	0.452±0.012
3 mg/ml	366.1±8.9	0.499±0.018
4 mg/ml	363.5±8.9	0.338±0.012

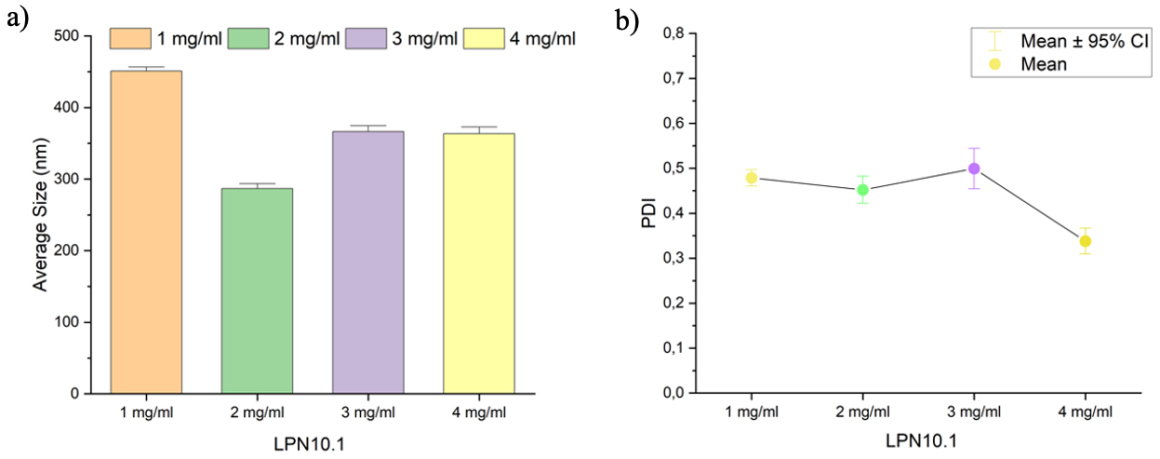

Figure 4.10 Graphs of BSA-Dextran Conjugate Concentration Effect on Liquid Lipid-Polymer Hybrid Nanoparticle a) Size b) PDI.

4.2.1.4 Purification Effect on Nanoparticle Size and Polydispersity

Different purification techniques were performed to obtain smaller sizes in nanoparticles and to smooth away the excessive materials (Table 4.8). Centrifugation resulted with bigger size, but smaller PDI in nanoparticle SLPN10.1 which could be because very small nanoparticles were stayed in the supernatant after centrifugation, while the bigger but similar sized nanoparticles were seperated as pellet. So; after three times centrifugation, we obtained slightly bigger sized, highly monodisperse nanoparticles. That's why centrifugation could be used to obtain more monodisperse nanoparticles. Syringe filter (pore size: 0.45 μm) usage after the centrifugation resulted with very small amount of solid content; so, it could not be measured up to 1 ml nanoparticle. Therefore, syringe filter usage after centrifugation was not a very effective way for nanoparticle purification. Syringe filter usage directly after the fabrication of nanopar-

ticles decreased both average size and polydispersity index of the nanoparticle. Also, only 15% of the solid content was decreased. So, syringe filter was a very effective way to reduce particle size and PDI without loss of big amounts of nanoparticles (Figure 4.11). As a result, syringe filtering method was chosen to be used in selected nanoparticle for purification.

Table 4.8 Purification Effect on Nanoparticle Size and PDI (Nanoparticle: SLPN10.1).

Purification Techniques	**Average Size (nm)**	**Polydispersity Index**	**Solid Content**
No purification	185.3±2.8	0.285±0.007	1 mg/ml
Centrifugation	238.8±3.1	0.214±0.004	0.25 mg/ml
Centrifugation + Syringe filter (450 nm)	155.9±1.5	0.095±0.011	Very low (Not measurable up to 1 ml dispersions)
Syringe filter (450 nm)	127.4±0.7	0.199±0.014	0.85 mg/ml

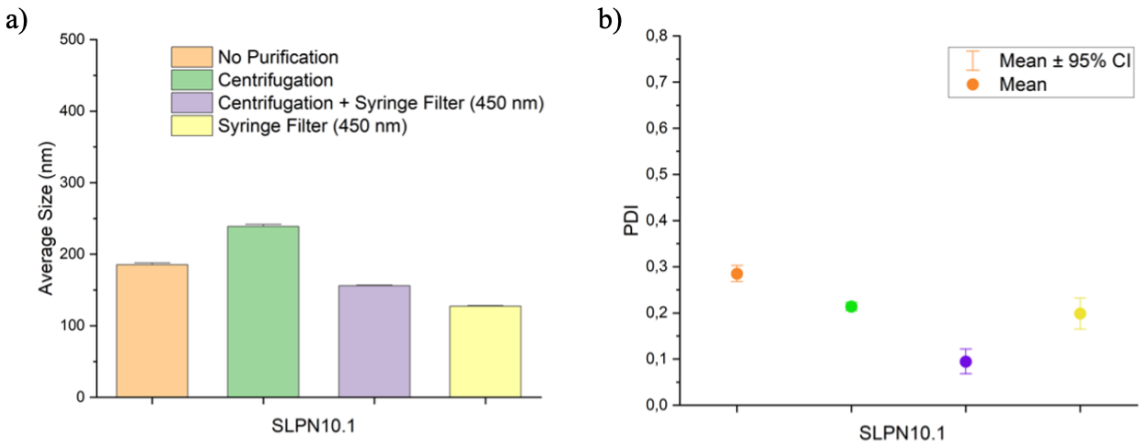

Figure 4.11 Graphs of Purification Effect on Nanoparticle a) Size b) PDI.

4.2.2 Selection of the Optimum Nanoparticle Design

As a result of the size and size distribution analysis given above, SLPN10.1 (Solid+Liquid Lipid-Polymer Hybrid Nanoparticle) (BSA:Dextran molar ratio: 1:1) was selected as the optimum nanoparticle for this thesis since it has the smallest size with narrow size distribution. Syringe filtered (pore size: 450 nm) image of the selected nanoparticle (Figure 4.12) and its size and zeta potential graph (Figure 4.13) could be seen below. The average size, zeta potential, and solid content of the syringe filtered SLPN10.1 was 127.4 nm, -41.8 mV, and 0.85 mg/ml, respectively.

Figure 4.12 Selected nanoparticle: SLPN10.1 (Syringe Filtered)

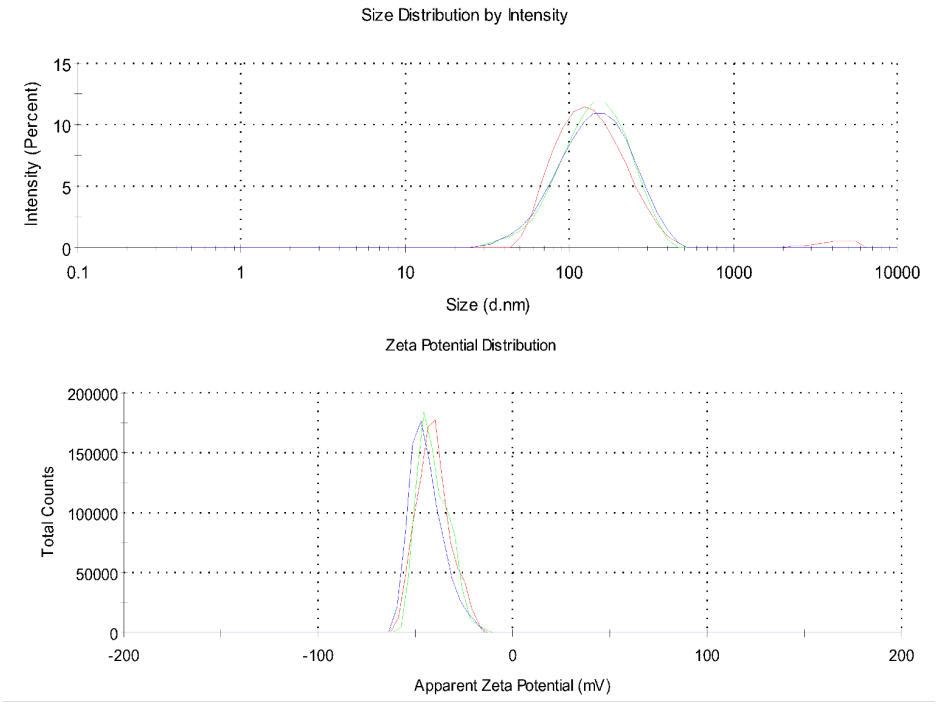

Figure 4.13 Size and zeta potential graphs of SLPN10.1

4.2.3 Stability Test Results

The size, size distributions, and zeta potential of the selected nanoparticle (SLPN10.1) were measured in day 0, day 84, and day 121 to check if the nanoparticle could stay stable in four months period (Table 4.9). Stability test results of the selected nanoparticle (SLPN10.1) showed that the nanoparticle size was not significantly changed in four months, and it was between 235 to 265 nm. Similarly, nanoparticle PDI was not significantly increased in that period, and it was between 0.380 to 0.420 (Figure 4.14). Also, the test results of the selected nanoparticle showed that the nanoparticle zeta potential was not significantly changed in four months, and it was between -39 to -43 mV (Figure 4.15). These results displayed that selected nanoparticle was stable for four months in terms of size, polydispersity index, and zeta potential.

Table 4.9 Stability test results of SLPN10.1 in terms of size, PDI, and zeta potential

Time (days)	Average Size (nm)	Polydispersity Index	Zeta Potential (mV)
0	254.4±7.4	0.380±0.011	-40.7±0.1
84	260.3±1.6	0.416±0.012	-39.1±0.4
121	237.9±3.1	0.405±0.007	-42.2±0.4

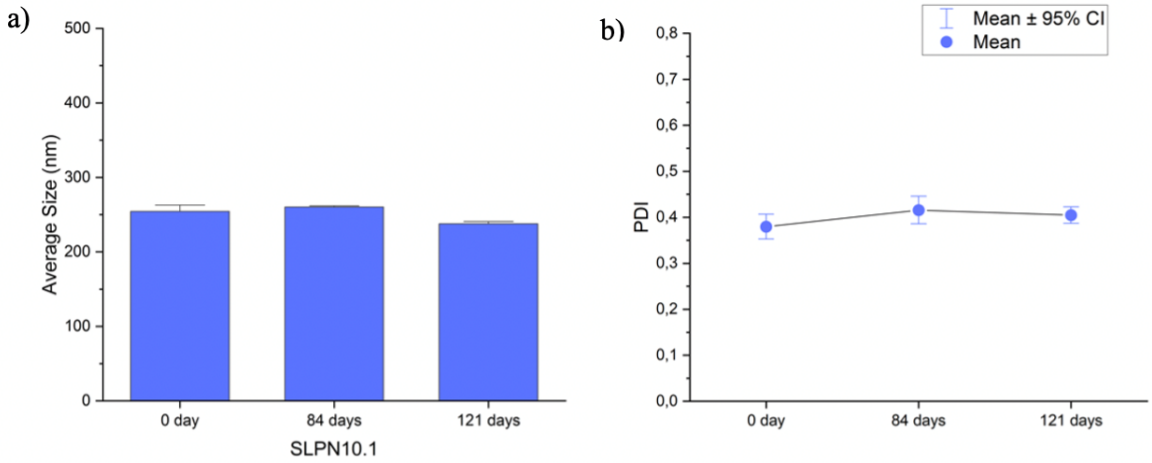

Figure 4.14 Graphs of stability tests for selected nanoparticle a) Size b) PDI.(Nanoparticle: SLPN10.1)

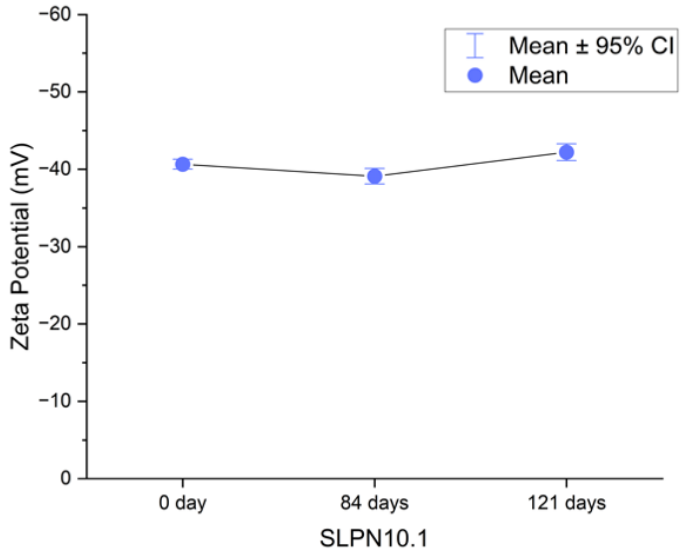

Figure 4.15 Graph of selected nanoparticle (SLPN10.1) stability in terms of zeta potential.

4.2.4 Zeta Potential Analysis

Two different zeta potential analysis were performed in this thesis. In the first analysis; zeta potential, size and size distribution of the selected nanoparticle (SLPN10.1) were measured in early endosomal and physiological pH along with its own natural pH. In the second analysis; zeta potential, size, and size distribution of SLPN10.1 were measured in nine different pH conditions which are from pH 2 to pH 10. The results of these analysis are given below.

4.2.4.1 Zeta Potential, Size and Size Distribution Analysis for Early Endosomal and Physiological Conditions

Nanoparticle average size and PDI were measured in early endosomal (pH 6.5), physiological (pH 7.4), and its own pH (pH 8) conditions (Table 4.10). Average sizes and PDI were between 200 to 240 and 0.185 to 0.230, respectively (Figure 4.16). Zeta potential of the nanoparticles in pH 6.5, 7.4, 8 were -18.5, -36.3, -36.4, respectively (Table 4.10). It could be seen that as the pH decreased, zeta potential becomes more positive which is expected since the nanoparticles in more acidic environment have more hydrogen ions, so that they have more positive charges (Figure 4.17). Moreover;

Table 4.10 Size, polydispersity index, and zeta potential analysis for early endosomal, physiological and its own pH conditions (Nanoparticle: SLPN10.1)

pH	Average Size (nm)	Polydispersity Index	Zeta Potential (mV)
6.5	226.4±36.8	0.207±0.116	-18.5±1.8
7.4	230.9±4.6	0.229±0.030	-36.3±0.4
8	205.7±1.6	0.185±0.023	-36.4±1.5

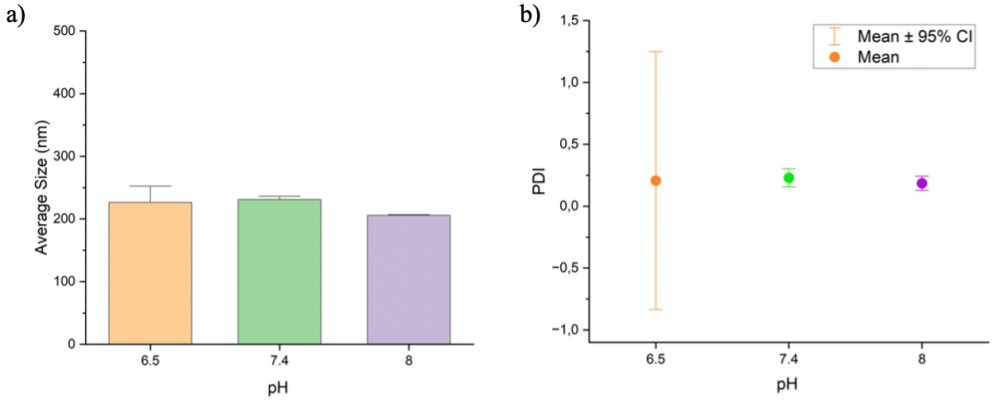

Figure 4.16 Graphs of selected nanoparticle's a) Size and b) PDI analysis for early endosomal, physiological and its own pH conditions (Nanoparticle: SLPN10.1)

it could be seen that while the nanoparticle was highy stable in physiological pH; in pH 6.5, zeta potential is around -20 which means the nanoparticle is unstable in this pH, and it means that around tumor site the nanoparticle shell structure could denaturate and nanoparticles can release an active agent to these sites.

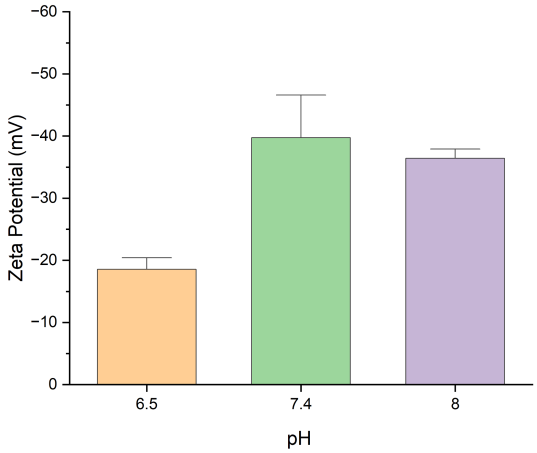

Figure 4.17 Graph of zeta potential results of the selected nanoparticle (SLPN10.1) in early endosomal, physiological and its own pH conditions.

4.2.4.2 pH Dependent Zeta Potential, Size, and Size Distribution Analysis of Selected Nanoparticle

The table of pH dependent zeta potential, size and size distribution analysis of selected nanoparticle (SLPN10.1) is given below (Table 4.11). According to zeta potential analysis result of selected nanoparticle (SLPN10.1) which could be seen in Figure 4.18, below pH 4; the nanoparticle had strong positive charges, above pH 4; it had strong negative charges. That means the isoelectric point of the nanoparticle is close to pH 4, which is logical because isoelectric point of BSA is between 4.5 and 4.8 and BSA is the predominant material in shell. Shell of the selected nanoparticle has BSA-Dextran10 conjugate with molar ratio of 1:1, thus, BSA amount is much higher than dextran in the nanoparticles since molecular weight of BSA (66.5 kDa) is much higher than molecular weight of Dextran10 (9 to 11 kDa). As zeta potential was higher than 30 (positively or negatively) in each pH condition except pH 4, the nanoparticle was electrostatically stable in those pH values.

It is also could be seen in Figure 4.19 that the selected nanoparticle size was

Table 4.11 pH Dependent zeta potential, size, and size distribution analysis of selected nanoparticle (SLPN10.1).

pH	Zeta Potential (mV)	Average Size (nm)	Polydispersity Index
2	41.7±0.6	202.1±2.0	0.257±0.003
3	37.4±0.5	187.6±0.9	0.259±0.004
4	-5.2±0.2	809.1±46.7	0.682±0.099
5	-36.5±1.2	189.0±4.1	0.260±0.011
6	-46.1±1.2	186.1±0.5	0.248±0.002
7	-43.7±0.0	199.4±0.4	0.297±0.055
8	-41.8±2.0	190.3±1.5	0.249±0.017
9	-47.4±0.5	189.5±1.7	0.243±0.014
10	-54.2±1.6	191.4±1.6	0.237±0.004

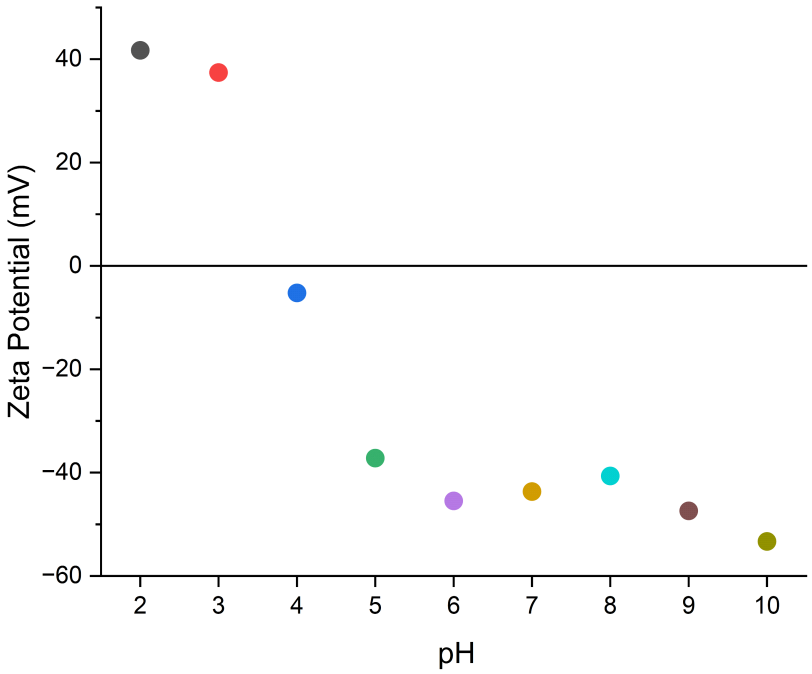

Figure 4.18 pH dependent zeta potential analysis of selected nanoparticle (SLPN10.1).

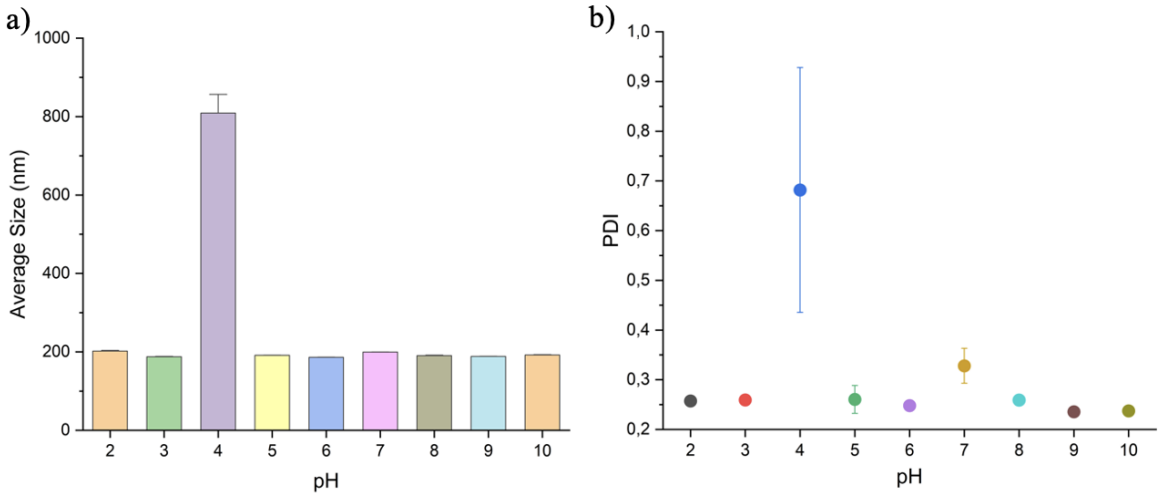

Figure 4.19 pH dependent (a) size, and (b) PDI analysis of selected nanoparticle (SLPN10.1).

very high in pH 4 which could be due to the precipitation of the nanoparticles since there was is no charge and as a conclusion there is not enough repulsion forces between nanoparticles in isoelectric point. In other pH values average sizes were between 185 and 203 nm. Besides, polydispersity index was also very high in pH 4. In other pH values PDI was between 0.230 and 0.300.

4.2.5 Morphological Characterization

The morphology of SLPN10.1 was imaged with STEM. As shown in Figure 4.20, the nanoparticles were spherical shaped and have a contrast between the core and surface of the nanoparticle. The particle size of the nanoparticle observed from STEM images was compatible with which obtained by DLS.

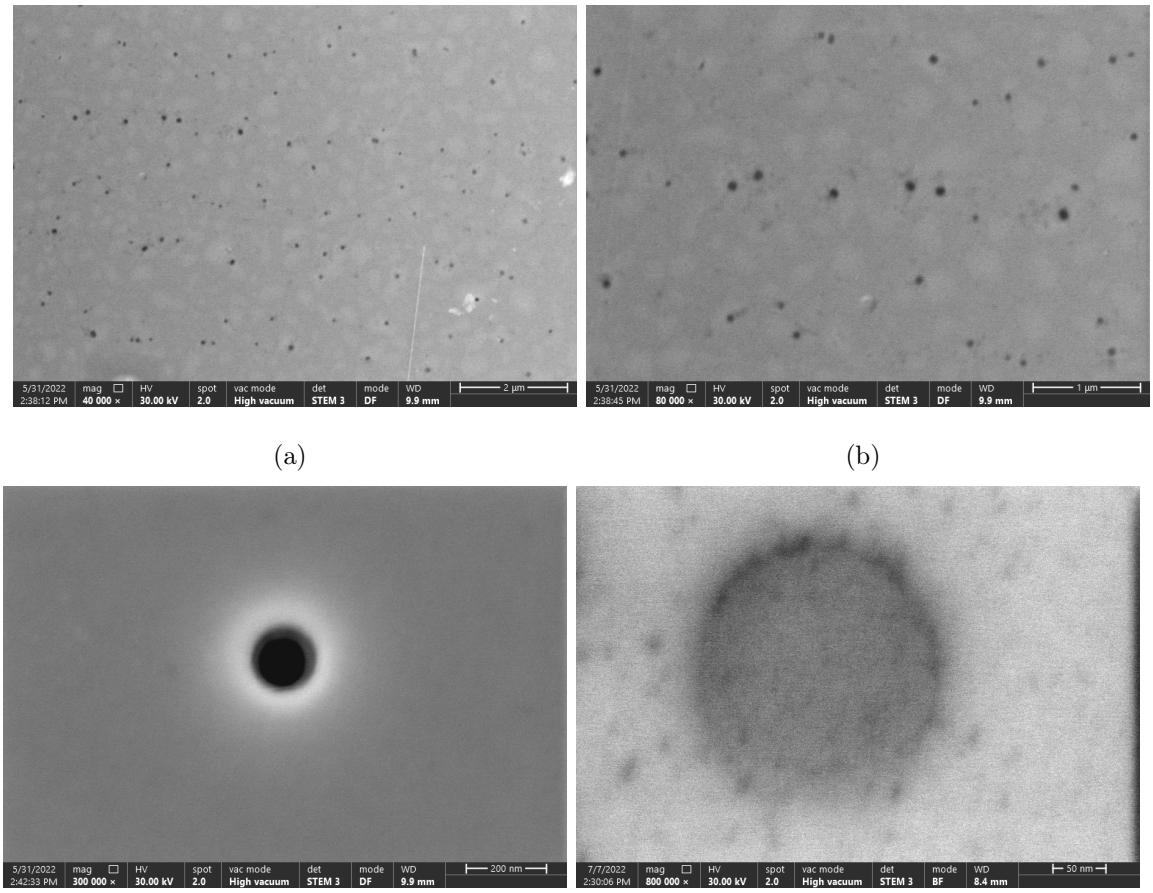

(a) (b)

(c) (d)

Figure 4.20 STEM (Scanning Transmission Electron Microscopy) images of selected nanoparticle (SLPN10.1) (a) scale: 2 µm, (b) scale: 1 µm, (c) scale: 200 nm , (d) scale: 50 nm.

5. CONCLUSIONS AND OUTLOOK

5.1 Conclusions

In this thesis, unique core-shell type lipid-polymer hybrid nanoparticles were fabricated. For shell of the nanoparticles BSA-Dextran conjugates were fabricated with Maillard reaction and characterized. Two different core types as nanostructured lipid core (solid lipid + liquid lipid) and liquid lipid core were used to compare their differences in terms of average size and PDI. Beeswax was used as solid lipid and olive oil was used as liquid lipid in the nanoparticles. According to performed experiments and characterizations, following results were observed:

1. BSA-Dextran conjugates served as an emulsifier to nanoparticles, so that; stable, small sized, narrowly distributed nanoparticles were obtained without use of a synthetic surface-active agent.

2. According to protein assay characterization of the Maillard conjugates, efficiency of protein concentrations was highest when protein-polysaccharide molar ratio was 1:1, and it decreased with increasing protein amount. There was only one exception; BSA;Dex10.3 (Protein-Polysaccharide molar ratio: 3:1) showed higher protein efficiency than other conjugates with Dextran10 that have smaller protein molar ratio. Protein efficiency according to BSA:Dextran molar ratio was 1:1 $>$ 2:1 $>$ 3:1.

3. SDS-PAGE and FTIR results confirmed the complexation of BSA and Dextran.

4. Preventing overheating of nanoparticles via ice usage around the experiment vials during ultrasonication process resulted with smaller sizes and narrower size distributions than experiments without ice. This could be because when the temperature was too high in no ice used experiments, the proteins were denaturating and the shell formation around the core were not properly performed, so that the nanoparticles aggregated together and caused high nanoparticle average sizes.

5. Different dextran molecular weights in shell of the nanoparticles did not result with significantly different average sizes and polydispersity indexes for both SLPNs and LPNs. However, minor increases can be seen in SLPNs average sizes as dextran molecular weights increase.

6. Changes in BSA-Dextran molar ratios (1:1, 2:1, 3:1) did not result with significantly different average sizes and polydispersity indexes for SLPNs.

7. Increase in Maillard conjugate concentrations in continuous phase resulted with increase in average size and decrease in polydispersity index for SLPNs. However, there was no ordered increase or decrease in average size or PDIs for LPNs. LPNs showed higher average sizes and wider size distributions than SLPNs.

8. Centrifugation increases average nanoparticle size, but results with smaller polydispersity indexes.

9. Syringe filtering (Pore size: 450 nm) the nanoparticles resulted with smaller nanoparticle size and PDI, and only 15% of the solid content lost in this process.

10. pH dependent zeta potential, size, and size distribution analysis showed that isoelectric point of the selected nanoparticle (SLPN10.1) was around pH 4, and the nanoparticle had strong positive or negative charges in other pH values.

11. In general, DLS results showed that average sizes and PDIs of fabricated SLPNs were between 200-260 nm and between 0.150-0.350, respectively.

12. STEM results confirmed the nanoparticle size outcomes obtained from DLS and showed well-constructed spherical shape of the nanoparticles.

13. Finally, SLPN10.1 was chosen for future drug loading and release experiments of this study because of its appropriate properties such as small size (Average size: 127.4 nm), narrow size distribution (PDI: 0.199), and long-term stability (4 months).

5.2 Outlook

The nanoparticle design produced in this study has potential to be a new nanodrug for lipophilic drug delivery. Therefore, Paclitaxel, which is a highly lipophilic anticancer drug, is planned to be used for drug encapsulation and release studies in the future projects. In drug encapsulation experiments, it is planned to achieve a drug loading rate of 0.1 mg/ml, based on the procedure in previous studies where Doxorubicin cancer drug encapsulation was performed [46], and considering the encapsulation amount in Paclitaxel-containing lipid nanoparticle studies in the literature [41] [47]. Furthermore, conducting drug release experiments with both passive targeting and enzymatic triggering is planned.

Besides, Polysorbate 20 (Tween 20) (IUPAC name: Polyoxyethylene (20) sorbitan monolaurate) could be used as a surfactant in the nanoparticles in future studies as control group to compare the stability of nanoparticles with surfactants and with only protein-polysaccharide complexes as stabilisers. Polysorbate 20 is a non-ionic surfactant. Primary advantages of non-ionic surfactants are their stability, non-toxicity, high therapeutic efficacy and easy handling and storage [48]. Also their considerably low cost is eligible for industrial manufacturing in both cosmetics and pharmaceutical administrations. Furthermore, their preparation for small-scale or large-scale production could be carried out without pharmaceutically undesired solvents [48]. Polysorbate 20, was used in many cosmetic products such as soups, detergents, and lotions. It is also used in foods such as milk creams. The main reason of choosing this surfactant for future studies of this project was its non-toxicity in low percentages (1-2 vol%).

Moreover, nanoparticle design in this thesis could be further improved with ligands to actively target cancer cells by ligand-receptor attachments. For this purpose, hyaluronic acid could be used as a ligand for CD44 receptors [49]. Furthermore, with small changes in the design, stimuli-responsive such as temperature or pH responsive nanoparticles could be produced.

REFERENCES

1. Wang, X., C. T. Ho and Q. Huang, "Investigation of adsorption behavior of (-)-epigallocatechin gallate on bovine serum albumin surface using quartz crystal microbalance with dissipation monitoring", *Journal of Agricultural and Food Chemistry*, Vol. 55, pp. 4987–4992, 6 2007.

2. Nadkar, S. and C. Lokhande, "Current trends in novel drug delivery - An OTC perspective", *Pharma Times*, Vol. 42, pp. 17–23, 04 2010.

3. Loxley, A., "Solid lipid nanoparticles for the delivery of pharmaceutical actives", *Drug Delivery Technology*, Vol. 9, pp. 32–37, 09 2009.

4. Mishra, B., B. B. Patel and S. Tiwari, "Colloidal nanocarriers: a review on formulation technology, types and applications toward targeted drug delivery", *Nanomedicine : nanotechnology, biology, and medicine*, Vol. 6, pp. 9–24, 2010.

5. Hossen, S., M. K. Hossain, M. K. Basher, M. N. Mia, M. T. Rahman and M. J. Uddin, "Smart nanocarrier-based drug delivery systems for cancer therapy and toxicity studies: A review", *Journal of Advanced Research*, Vol. 15, pp. 1–18, 1 2019.

6. Anarjan, F. S., "Active targeting drug delivery nanocarriers: Ligands", *Nano-Structures Nano-Objects*, Vol. 19, p. 100370, 7 2019.

7. Torchilin, V. P., "CHAPTER 1 Fundamentals of Stimuli-responsive Drug and Gene Delivery Systems", pp. 1–32, 7 2018.

8. Matsumura, Y. and H. Maeda2, "A New Concept for Macromolecular Therapeutics in Cancer Chemotherapy: Mechanism of Tumoritropic Accumulation of Proteins and the Antitumor Agent Smancs1", , 1986.

9. Mukherjee, S., S. Ray and R. S. Thakur, "Solid Lipid Nanoparticles: A Modern Formulation Approach in Drug Delivery System", *Indian Journal of Pharmaceutical Sciences*, Vol. 71, p. 349, 2 2009.

10. Gordillo-Galeano, A. and C. E. Mora-Huertas, "Solid lipid nanoparticles and nanostructured lipid carriers: A review emphasizing on particle structure and drug release", *European Journal of Pharmaceutics and Biopharmaceutics*, Vol. 133, pp. 285–308, 12 2018.

11. Westesen, K., H. Bunjes and M. H. Koch, "Physicochemical characterization of lipid nanoparticles and evaluation of their drug loading capacity and sustained release potential", *Journal of Controlled Release*, Vol. 48, pp. 223–236, 10 1997.

12. Pardeike, J., A. Hommoss and R. H. Müller, "Lipid nanoparticles (SLN, NLC) in cosmetic and pharmaceutical dermal products", *International Journal of Pharmaceutics*, Vol. 366, pp. 170–184, 1 2009.

13. Duan, Y., A. Dhar, C. Patel, M. Khimani, S. Neogi, P. Sharma, N. S. Kumar and R. L. Vekariya, "A brief review on solid lipid nanoparticles: part and parcel of contemporary drug delivery systems", *RSC Advances*, Vol. 10, pp. 26777–26791, 7 2020.

14. Jenning, V., A. F. T. N. B and S. H. Gohla, "Characterisation of a novel solid lipid nanoparticle carrier system based on binary mixtures of liquid and solid lipids", , 2000.

15. Joshi, M. D. and R. H. Müller, "Lipid nanoparticles for parenteral delivery of actives", *European journal of pharmaceutics and biopharmaceutics : official journal of Arbeitsgemeinschaft fur Pharmazeutische Verfahrenstechnik e.V*, Vol. 71, pp. 161–172, 2 2009.

16. Müller, R. H., R. D. Petersen, A. Hommoss and J. Pardeike, "Nanostructured lipid carriers (NLC) in cosmetic dermal products", *Advanced Drug Delivery Reviews*, Vol. 59, pp. 522–530, 7 2007.

17. Beloqui, A., M. Ángeles Solinís, A. Rodríguez-Gascón, A. J. Almeida and V. Préat, "Nanostructured lipid carriers: Promising drug delivery systems for future clinics", *Nanomedicine : nanotechnology, biology, and medicine*, Vol. 12, pp. 143–161, 1 2016.

18. Alasvand, N., A. M. Urbanska, M. Rahmati, M. Saeidifar, P. S. Gungor-Ozkerim, F. Sefat, J. Rajadas and M. Mozafari, "Therapeutic Nanoparticles for Targeted Delivery of Anticancer Drugs", *Multifunctional Systems for Combined Delivery, Biosensing and Diagnostics*, pp. 245–259, 1 2017.

19. Hadinoto, K., A. Sundaresan and W. S. Cheow, "Lipid–polymer hybrid nanoparticles as a new generation therapeutic delivery platform: A review", *European Journal of Pharmaceutics and Biopharmaceutics*, Vol. 85, pp. 427–443, 11 2013.

20. Mandal, B., H. Bhattacharjee, N. Mittal, H. Sah, P. Balabathula, L. A. Thoma and G. C. Wood, "Core–shell-type lipid–polymer hybrid nanoparticles as a drug delivery platform", *Nanomedicine: Nanotechnology, Biology and Medicine*, Vol. 9, pp. 474–491, 5 2013.

21. Zhang, R., C. Wu, L. Tong, B. Tang and Q. H. Xu, "Multifunctional core-shell nanoparticles as highly efficient imaging and photosensitizing agents", *Langmuir*, Vol. 25, pp. 10153–10158, 9 2009.

22. Wu, W., J. Shen, Z. Gai, K. Hong, P. Banerjee and S. Zhou, "Multi-functional core-shell hybrid nanogels for pH-dependent magnetic manipulation, fluorescent pH-sensing, and drug delivery", *Biomaterials*, Vol. 32, pp. 9876–9887, 12 2011.

23. Wang, Y., K. Kho, W. S. Cheow and K. Hadinoto, "A comparison between spray drying and spray freeze drying for dry powder inhaler formulation of drug-loaded lipid–polymer hybrid nanoparticles", *International Journal of Pharmaceutics*, Vol. 424, pp. 98–106, 3 2012.

24. Bouyer, E., G. Mekhloufi, V. Rosilio, J.-L. Grossiord and F. Agnely, "Proteins, polysaccharides, and their complexes used as stabilizers for emulsions: Alternatives to synthetic surfactants in the pharmaceutical field?", *International journal of pharmaceutics*, Vol. 436, pp. 359–78, 06 2012.

25. Wang, T., M. Bae, J. Y. Lee and Y. Luo, "Solid lipid-polymer hybrid nanoparticles prepared with natural biomaterials: A new platform for oral delivery of lipophilic bioactives", *Food Hydrocolloids*, Vol. 84, pp. 581–592, 11 2018.

26. Rosen, J. T. K. M. J., "Surfactants and Interfacial Phenomena (4th ed.). Hoboken, New Jersey: John Wiley Sons.", pp. 33–34, 2012.

27. Belhaj, A. F., K. A. Elraies, S. M. Mahmood, N. N. Zulkifli, S. Akbari and O. S. E. Hussien, "The effect of surfactant concentration, salinity, temperature, and pH on surfactant adsorption for chemical enhanced oil recovery: a review", *Journal of Petroleum Exploration and Production Technology*, Vol. 10, pp. 125–137, 1 2020.

28. Friberg, S. E., "A review of " Surfactants and Polymers in Aqueous Solution " B.Jonsson, B.Lindman, K.Holmberg, B.Kronberg, Eds. John Wiley Sons, England, 1998.", *Journal of Dispersion Science and Technology*, Vol. 20, pp. 1285–1285, 6 2007.

29. Sekhon, B. S., "Surfactants: Pharmaceutical and Medicinal Aspects", *Journal of Pharmaceutical Technology, Research and Management*, Vol. 1, pp. 43–68, 5 2013.

30. McClements, D. J., "Protein-stabilized emulsions", *Current Opinion in Colloid Interface Science*, Vol. 9, No. 5, pp. 305–313, 2004.

31. Dickinson, E., "Hydrocolloids as emulsifiers and emulsion stabilizers", *Food Hydrocolloids*, Vol. 23, No. 6, pp. 1473–1482, 2009, 9th International Hydrocolloids Conference.

32. Shewach, D. S. and R. D. Kuchta, "Introduction to cancer chemotherapeutics", *Chemical reviews*, Vol. 109, pp. 2859–2861, 7 2009.

33. Thurston, D. E., "Chemistry and pharmacology of anticancer drugs", *British Journal of Cancer*, Vol. 97, p. 1713, 12 2007.

34. Wani, M. C., H. L. Taylor, M. E. Wall, P. Coggon and A. T. Mcphail, "Plant Antitumor Agents.VI.The Isolation and Structure of Taxol, a Novel Antileukemic and Antitumor Agent from Taxus brevifolia2", *Journal of the American Chemical Society*, Vol. 93, pp. 2325–2327, 5 1971.

35. Wang, T., J. Xue, Q. Hu, M. Zhou, C. Chang and Y. Luo, "Synthetic surfactant- and cross-linker-free preparation of highly stable lipid-polymer hybrid nanoparticles as potential oral delivery vehicles", *Scientific Reports*, Vol. 7, 12 2017.

36. "Fisher Scientific", `https://www.fishersci.se/se/en/home.html`.

37. Singla, A. K., A. Garg and D. Aggarwal, "Paclitaxel and its formulations", , 2002.

38. Paik, P. K., L. P. James, G. J. Riely, C. G. Azzoli, V. A. Miller, K. K. Ng, C. S. Sima, R. T. Heelan, M. G. Kris, E. Moore and N. A. Rizvi, "A phase 2 study of weekly albumin-bound paclitaxel (Abraxane ®) given as a two-hour infusion", *Cancer Chemotherapy and Pharmacology*, Vol. 68, pp. 1331–1337, 11 2011.

39. Rowinsky, E. K. and R. C. Donehower, "Taxol: Twenty Years Later, the Story Unfolds", *JNCI: Journal of the National Cancer Institute*, Vol. 83, pp. 1778–1781, 12 1991.

40. Danhier, F., N. Lecouturier, B. Vroman, C. Jérôme, J. Marchand-Brynaert, O. Feron and V. Préat, "Paclitaxel-loaded PEGylated PLGA-based nanoparticles: In vitro and in vivo evaluation", *Journal of Controlled Release*, Vol. 133, pp. 11–17, 1 2009.

41. Dong, X., C. A. Mattingly, M. Tseng, M. Cho, V. R. Adams and R. J. Mumper, "Development of new lipid-based paclitaxel nanoparticles using sequential simplex optimization", *European Journal of Pharmaceutics and Biopharmaceutics*, Vol. 72, pp. 9–17, 5 2009.

42. Sinha, V. R., A. K. Singla, S. Wadhawan, R. Kaushik, R. Kumria, K. Bansal and S. Dhawan, "Chitosan microspheres as a potential carrier for drugs", *International Journal of Pharmaceutics*, Vol. 274, pp. 1–33, 4 2004.

43. Landfester, K. and V. Mailänder, "Nanocapsules with specific targeting and release properties using miniemulsion polymerization", *Expert Opinion on Drug Delivery*, Vol. 10, pp. 593–609, 5 2013.

44. Bautista, M. C., O. Bomati-Miguel, M. D. P. Morales, C. J. Serna and S. Veintemillas-Verdaguer, "Surface characterisation of dextran-coated iron oxide nanoparticles prepared by laser pyrolysis and coprecipitation", *Journal of Magnetism and Magnetic Materials*, Vol. 293, pp. 20–27, 5 2005.

45. Jian, W., J. He, Y. Sun and J. Pang, "Comparative studies on physicochemical properties of bovine serum albumin-glucose and bovine serum albumin-mannose conjugates formed via Maillard reaction", *LWT - Food Science and Technology*, Vol. 69, pp. 358–364, 6 2016.

46. Iyisan, B., J. Kluge, P. Formanek, B. Voit and D. Appelhans, "Multifunctional and Dual-Responsive Polymersomes as Robust Nanocontainers: Design, Formation by Sequential Post-Conjugations, and pH-Controlled Drug Release", *Chemistry of Materials*, Vol. 28, No. 5, pp. 1513–1525, 2016.

47. Zhai, J., R. B. Luwor, N. Ahmed, R. Escalona, F. H. Tan, C. Fong, J. Ratcliffe, J. A. Scoble, C. J. Drummond and N. Tran, "Paclitaxel-Loaded Self-Assembled Lipid Nanoparticles as Targeted Drug Delivery Systems for the Treatment of Aggressive Ovarian Cancer", *ACS Applied Materials & Interfaces*, Vol. 10, No. 30, pp. 25174–25185, 2018.

48. Marzio, L. D., S. Esposito, F. Rinaldi, C. Marianecci and M. Carafa, "Polysorbate 20 vesicles as oral delivery system: In vitro characterization", *Colloids and Surfaces B: Biointerfaces*, Vol. 104, pp. 200–206, 4 2013.

49. Zhao, Q., J. Liu, W. Zhu, C. Sun, D. Di, Y. Zhang, P. Wang, Z. Wang and S. Wang, "Dual-stimuli responsive hyaluronic acid-conjugated mesoporous silica for targeted delivery to CD44-overexpressing cancer cells", *Acta Biomaterialia*, Vol. 23, pp. 147–156, 9 2015.

APPENDIX A. STANDARD CURVE FOR PROTEIN ASSAY

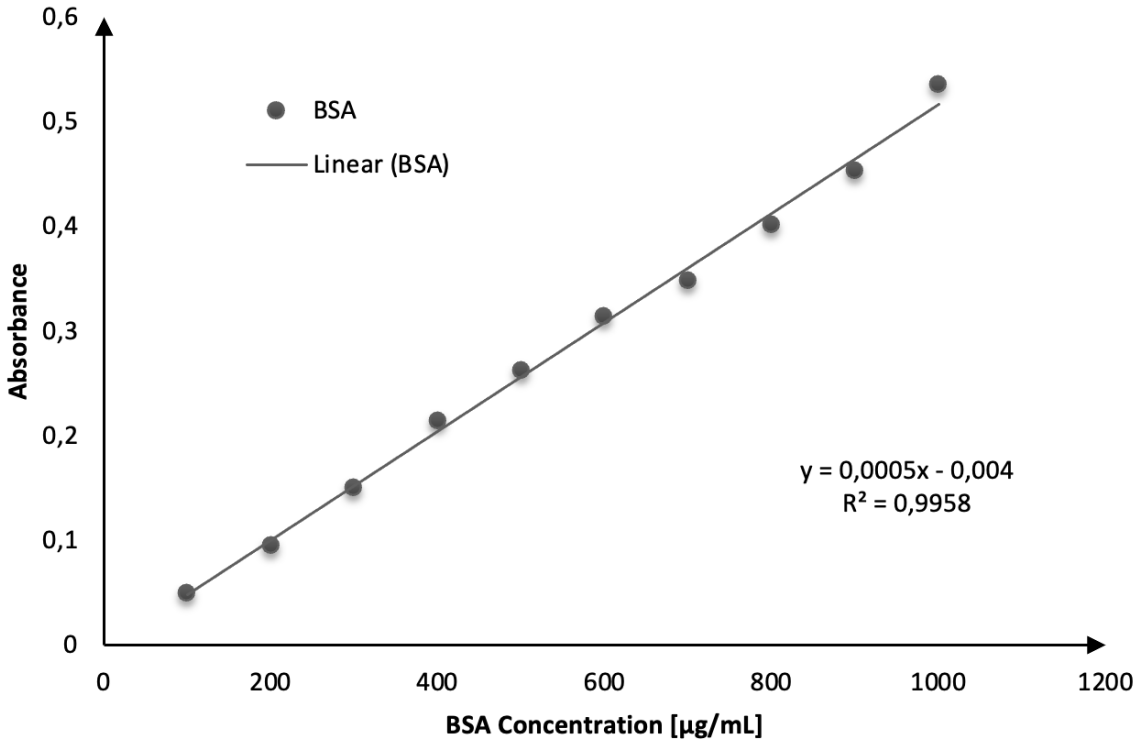

Figure A.1 Calibration Curve of BSA determined from absorbance values at $\lambda = 655$ nm to calculate protein concentrations of each Maillard complex.